CHAPTER EIGHT

General Comments and Suggestions for Further Work

From an investigation of a whole series of oxide dispersion strengthened alloys, it is evident that a highly anisotropic grain structure can be achieved either by directional recrystallisation of a "cold-deformed" microstructure, or by directional grain growth (secondary recrystallisation) in an ultra fine grained microstructure generated by primary recrystallisation. In the latter case, the process is more amenable to control since the driving force is lower. In cases where the particle distribution is anisotropic, directional recrystallisation could be achieved even during isothermal annealing, but the direction of recrystallisation was found to be impossible to control.

The behaviour of all the alloys could be rationalised in terms of their starting microstructure and processing conditions. Furthermore, the zone annealing conditions could be broadly rationalised in terms of the concept of kinetic strength, although much further work is needed to interpret parameters such as the activation energy.

There are some exciting possibilities in the design of such alloys. It would be interesting deliberately create highly anisotropic and controlled particle dispersions to induce directional recrystallisation or grain growth along particular desired path. A further modification could include particles which are not only aligned, but which are themselves anisotropic (e.g., plate shaped), thereby giving an anisotropic pinning effect.

From a theoretical point of view, it is necessary to further develop the concept of kinetic strength to include its dependence on stored energy, but this will require the availability of a good high temperature differential scanning calorimeter.

APPENDIX ONE

Zone Annealing and Isothermal Annealing Experiments Performed on Rapidly Solidified Aluminium Alloys Al-5 and Al-15

9.1 Introduction

The first attempts to produce directional recrystallisation were actually made on the alloys discussed below, but they did not turn out to be very successful. Some useful results were nevertheless obtained and are documented below.

Aluminium alloys are currently being developed, using the concepts of rapid solidification technology (RST), for applications to temperatures as high as 350°C (Thomas et al., 1986).

The applications of rapid solidification technology to aluminium alloys has led to two important developments: firstly, the achievement of a highly refined microstructure, elimination of coarse intermetallics and improved tolerance to impurity elements; and secondly, a large increase in the range and quantity of alloying elements which can be used in solid solutions (Couper, 1984).

With the aim of obtaining more data for the model of directional recrystallisation, zone annealing and isothermal annealing experiments were also performed on the low density aluminium alloys produced by rapid solidification technology, designated as Al-5 (Al-4.82Cr-1.40Zr-1.41Mn wt%, air-atomised) and Al-15 (Al-5.20Cr-1.89Zr-0.96Mn wt%, nitrogen-atomised). The chromium and zirconium additions, which are forced into solution by rapid solidification, lead eventually to the formation of highly stable intermetallics, giving a system with a large fraction of precipitated dispersoids. The work presented below is however, incomplete, since enormous difficulties were encountered in thin foil preparation and achieving high temperature gradients.

9.2 Zone Annealing

The specimens were prepared by swaging the alloys down to a 3 mm diameter rod at ambient temperature. After cold working, the specimens were finally cut to 20 mm lengths. To observe the changes in properties, hardness measurements were made in the as-received condition and after deformation. The hardness measured for alloy Al-5 prior to and after deformation turned out as 40 and 106 HVN(5kg) respectively and for alloy Al-15 as 65 and 117 HVN(5kg) respectively. The

light microscope and transmission electron micrographs taken for the as-received condition and after deformation are shown in figures 9.1-3 and are consistent with the hardness results stated above.

From the figure 9.1a and c, it can be seen that, the alloy Al-5 has a coarse grain structure in the as-received condition relative to alloy Al-15, The starting grain size is in these materials determined by the atomisation process; the finer particle size and higher chromium and zirconium contents of Al-15 are consistent with the higher hardness of this alloy when compared with Al-5 before and after deformation. Figures 9.1-3 illustrate the severe change in microstructure due to deformation. The as-received samples seem to contain a non-random distribution of particles with an expected higher particle density in Al-15.

The temperature cycle experienced at a point on the specimen, for different speeds, from 1.4 mm/min, 3.2 mm/min and 5.0 mm/min, and for different peak temperatures ranging from 200 to 600°C are shown in figure 9.4.

The effect of the zone annealing treatments on the deformed samples is shown in figure 9.5. Zone annealing with T_p = 200°C (T_p is the peak temperature) produced no significant change relative to the grain structure shown in longitudinal section. From the high hardness values (Table 9.1a), it is quite clear that for T_p at or below 200°C, the zone annealing treatment does not significantly influencing the microstructure of alloy Al-5. But for the same alloy zone annealing at T_p = 600°C a remarkable change is apparent, accompanied by a large drop in hardness (figure 9.5). The grains are elongated their very low hardness is encouraging since it indicates directional recrystallisation, although the microstructure could in principle be produced by recovery on its own; much further confirmation is required. Optical micrographs for alloy Al-15 (figure 9.6), zone annealed with T_p = 200 and 600°C, illustrate significant changes in grain structure, even for T_p = 200°C, consistent with the lower fraction of dispersoids.

Table 9.1a. Microstructure and Vickers hardness data obtained for Alloy Al-5, after zone-anneal
and 400 ^{0}C with different specimen travel speeds. Hardnesses measured in the as-recei
deformation (an 70% reduction by cold-swaging) were 38 and 106 HVN(5kg) respec

T_P ^{0}C	Specimen	Specimen Travel Speed mm/min			Hardness Vickers HVN(5kg)			Mear
	Condition	1.4	3.2	5.0	1.4	3.2	5.0	1
200	PI: SD	D	D	D	102	96	107	1
					102	103	107	
					102	103	106	
					101	105	105	
					101	104	104	
300	PI:SD	D	D	D	102	102	101	8
					101	102	100	
					99	100	102	
					97	102	102	
					97	99	97	
400	PI:SD	D	D	D	100	102	100	1
					102	104	103	
					100	102	102	
					100	105	101	
					100	100	101	

Table 9.1a. Microstructure and Vickers hardness data obtained for Alloy Al-5, after zone-annealing 500 and 600 ^{0}C with different specimen travel speeds.

T_P ^{o}C	Specimen Condition	Specimen Travel Speed mm/min 1.4	3.2	5.0	Hardness Vickers HVN(5kg) 1.4	3.2	5.0	Mean Hard 1.4
500	PI:SD	D	D	D	66	88	89	71
					72	87	89	
					75	86	88	
					71	86	82	
					73	87	82	
600	PI:SD	D	D	D	43	70	61	52
					52	71	63	
					52	70	69	
					60	73	67	
					54	72	49	

Table 9.1b. Microstructure and Vickers hardness data obtained for Alloy Al-15, after zone-annealin
and 400 ^{0}C with different specimen travel speeds. Hardnesses measured in the as-receiv
deformation (an 70% reduction by cold-swaging) were 65 and 113 HVN(5kg) respecti

T_P ^{0}C	Specimen	Specimen Travel Speed mm/min			Hardness Vickers HVN(5kg)			Mean Ha
	Condition	1.4	3.2	5.0	1.4	3.2	5.0	1.4
200	PI: SD	D	D	D	104	107	107	106
					107	109	108	
					107	109	108	
					106	108	109	
					103	105	107	
300	PI:SD	D	D	D	104	103	104	83
					104	104	105	
					104	104	104	
					104	102	106	
					91	104	91	
400	PI:SD	D	D	D	110	105	109	108
					109	113	112	
					108	114	110	
					108	112	114	
					105	194	98	

Table 9.1b. Microstructure and Vickers hardness data obtained for Alloy Al-15, after zone-annealin
500 and 600 ^{0}C with different specimen travel speeds.

T_P ^{o}C	Specimen Condition	Specimen Travel Speed mm/min 1.4	3.2	5.0	Hardness Vickers HVN(5kg) 1.4	3.2	5.0	Mean H 1.4
500	Pl:SD	D	D	D	95	107	111	97
					100	109	113	
					100	110	110	
					100	108	112	
					92	108	110	
600	Pl:SD	D	D	D	88	94	93	88
					88	95	90	
					89	93	91	
					86	87	91	
					88	87	90	

9.3 Isothermal Annealing

Isothermal annealing experiments were performed on both Al-5 and Al-15, using conventional furnaces. The specimens were annealed at temperatures ranging from 200 to 550°C, at 50°C intervals. They were kept in furnaces for a total time of 3687200 seconds; the first specimen was annealed for 900 seconds, and the time at temperature was doubled for each successive sample. The hardness data are listed in Table 9.2a-b.

An aim of these experiments was to see whether the hardness changes during isothermal annealing could be rationalised using a simple Avrami approach, in which case it might be possible to subsequently rationalise changes during anisothermal annealing. We first define ζ as a function representating recovery or recrystallisation

$$\zeta = (H_{max} - H) / (H_{max} - H_{min}) \qquad .....(9.1)$$

where

H = hardness of the material at any instant of time,

H_{max} = maximum hardness of specimen after deformation,

H_{min} = minimum hardness of specimen after annealing,

ζ = 1, when the specimen is fully annealed,

ζ = 0, when the specimen is in deformed condition.

Therefore $\zeta = f\{ t , T \}$, and T = absolute temperature.

Until the detailed microstructural studies give information about the mechanism of change in hardness, an Avrami (1939, 40 & 41) relation is assumed for the analysis of isothermal curves;

$$\zeta = 1 - \exp \{-kt^n\} \qquad .....(9.2)$$

where

n = exponent

k = rate constant = $k_0 \exp (- Q/RT)$

Q = activation energy for the recovery or recrystallisation processes.

The relation is intuitively expected to be correct if for example recrystallisation governs hardness changes. Rearranging equation 9.2, we get

$$\ln (1 - \zeta) = -kt^n \qquad .....(9.3)$$

and finally we get,

$$\ln [- \ln (1 - \zeta)] = \ln k + n \ln t \qquad .....(9.4)$$

where the slope of graph is equal to n and the intercept = lnk.

Many graphs have been plotted in the above form, for different temperatures ranging from 200 to 500°C, as shown in figures 9.7 and 8. From figures 9.7 and 8, it can be seen that, at low temperatures ranging from 200 to 500°C, the hardness results measured for the isothermally annealed specimens of both the aluminium alloys Al-5 and Al-15, are less well behaved, when compared with the higher temperature data in figure 9.7 and 8, where the data fit the Avrami relation. It was not possible to find unique values of the Avrami parameters to adequately represent all data, indicating that equation 9.4 is invalid and that the approach needs modification after detailed studies of the changes occuring during annealing.

From the hardness results listed in Table 9.2a-b, it can be seen that on annealing the specimens at relatively low temperatures the hardness increases after annealing for 7200 seconds. This increase in hardness was detected even at longer times, but at the temperatures ranging from 300 to 350°C, only a very slight increase in hardness was obtained. At high temperatures ranging from 500 to 550°C, a continuous decrease in hardness was recorded, finally reaching the hardness of the material measured in the as-received condition. This increase in hardness at low temperatures was observed for both aluminium alloys Al-5 and Al-15, and is presumably due to precipitation induced age hardening as reported by Miller et al., (1985): the hardness results observed are graphically shown in figure 9.9.

Optical micrography (figures 9.10 & 9.11) revealed no significant change in microstructure at low annealing temperatures. In figure 9.11, micrographs are illustrated for alloys Al-5 and Al-15, annealed at high temperature (i.e., 550°C). The hardness measured at high temperatures, even after short time treatment was rather low, and an obvious change in microstructure is apparent, which can be seen from figure 9.11a-c, where the grains are elongated even though the hardness has dropped drastically. As noted earlier, this may indicate directional recrystallisation but this needs to be confirmed using transmission electron microscope.

Table 9.2a. Hardness data obtained for aluminium alloy Al-5 after isothermally annealing at 200 for the time periods ranging from 900 to 3687200 seconds.

T_p °C	ANNEALING TIME IN SECONDS										
	900	1800	3600	7200	14400	28800	57600	115200	230400	460800	9216
	HARDNESS HVN (5kg)										
200	113	117	109	99	98	95	102	104	98	98	95
	113	114	103	98	97	98	104	103	100	97	97
	113	113	103	102	98	100	102	106	97	95	96
	112	113	104	100	100	100	102	104	98	97	98
	114	113	104	97	99	97	93	102	98	94	96
	MEAN HARDNESS HVN (5kg)										
	113	114	105	99	98	98	101	104	98	96	97
250	114	112	111	118	124	124	118	117	125	114	113
	115	111	105	124	127	125	119	120	126	117	118
	112	110	111	124	128	124	120	125	127	116	117
	111	107	111	124	128	124	120	123	124	115	117
	107	109	109	117	124	110	118	119	107	115	114
	MEAN HARDNESS HVN(5kg)										
	112	110	109	121	126	121	119	121	122	115	116
300	111	103	106	98	102	98	97	99	98	111	116
	108	103	108	98	100	98	98	96	96	114	118
	101	101	110	98	100	95	100	95	100	115	115
	103	102	110	100	102	97	102	99	98	119	115
	102	100	110	100	100	95	97	96	95	124	110
	MEAN HARDNESS HVN(5kg)										
	105	102	109	99	101	97	99	97	98	117	115
350	93	98	104	101	96	92	93	91	91	115	111
	93	103	107	96	95	95	96	95	92	117	108
	98	107	100	98	96	93	96	93	92	118	108
	100	103	102	102	98	96	96	92	84	119	104
	114	103	109	97	93	92	93	93	84	110	108
	MEAN HARDNESS HVN(5kg)										
	100	103	104	99	96	93	95	93	88	116	108

Table 9.2a. Hardness data obtained for aluminium alloy Al-5 after isothermally annealing at 400, 450
for the time periods ranging from 900 to 3687200 seconds.

T_p ^0C	ANNEALING TIME IN SECONDS										
	900	1800	3600	7200	14400	28800	57600	115200	230400	460800	921600
	HARDNESS HVN (5kg)										
400	101	99	92	86	84	89	85	84	83	77	75
	101	98	83	88	85	87	88	84	82	79	79
	98	98	91	86	88	88	86	84	83	80	79
	101	96	93	90	86	83	86	84	83	80	79
	104	96	88	89	84	85	86	83	81	77	77
	MEAN HARDNESS HVN (5kg)										
	101	97	89	88	85	86	86	83	82	79	78
450	87	76	80	75	77	75	73	71	68	66	64
	86	79	83	77	78	75	74	72	67	64	65
	89	77	80	78	78	78	74	68	65	61	64
	90	78	81	80	79	76	74	69	68	59	66
	80	83	83	76	78	76	75	64	67	57	60
	MEAN HARDNESS HVN(5kg)										
	86	79	81	77	78	76	74	69	67	62	64
500	78	70	75	68	58	65	63	63	61	43	50
	77	74	73	67	60	67	63	62	62	53	53
	79	74	73	68	65	68	64	60	59	49	53
	78	77	73	67	64	64	65	61	60	52	48
	78	73	70	68	64	66	66	55	55	52	43
	MEAN HARDNESS HVN(5kg)										
	78	74	73	67	62	66	64	60	60	50	49
550	80	72	60	54	56	51	56	46	42	52	44
	77	69	63	62	59	49	56	46	45	46	40
	75	70	66	58	55	52	53	46	49	41	42
	71	70	67	56	52	48	54	44	47	42	43
	72	68	65	60	51	50	51	44	46	44	43
	MEAN HARDNESS HVN(5kg)										
	75	70	64	58	54	50	54	45	46	45	42

Table 9.2b. Hardness data obtained for aluminium alloy Al-15 after isothermally annealing at 200
for the time periods ranging from 900 to 3687200 seconds.

T_p °C	ANNEALING TIME IN SECONDS										
	900	1800	3600	7200	14400	28800	57600	115200	230400	460800	92160
	HARDNESS HVN (5kg)										
200	108	117	115	107	102	109	108	104	108	108	111
	113	119	116	110	107	110	108	109	108	107	112
	114	117	114	111	107	110	110	109	104	107	114
	112	117	113	110	107	110	109	104	100	107	110
	112	117	113	109	107	107	107	104	103	103	109
	MEAN HARDNESS HVN (5kg)										
	111	117	114	109	106	109	108	106	105	106	111
250	110	112	113	110	107	102	107	110	110	131	125
	111	111	113	108	107	107	110	110	110	132	133
	110	112	114	108	107	107	110	108	110	131	135
	110	113	113	107	107	103	110	109	109	130	134
	112	113	113	106	107	100	110	109	107	123	132
	MEAN HARDNESS HVN(5kg)										
	111	112	113	108	107	104	109	109	109	129	132
300	119	113	117	104	108	113	109	110	110	132	132
	116	113	116	104	110	114	108	110	112	138	138
	116	113	114	104	110	113	106	111	113	137	138
	117	116	114	104	110	111	109	110	111	137	139
	109	116	114	105	114	115	107	109	107	136	136
	MEAN HARDNESS HVN(5kg)										
	115	114	115	104	110	113	108	110	111	136	137
350	113	117	117	113	107	113	110	113	112	133	124
	112	118	116	112	110	115	113	113	114	135	133
	113	115	117	112	111	110	112	112	115	132	131
	113	116	119	110	110	114	114	110	114	134	131
	115	117	118	111	110	115	111	99	110	126	127
	MEAN HARDNESS HVN(5kg)										
	113	117	117	112	110	113	112	109	113	132	129

Table 9.2b. Hardness data obtained for aluminium alloy Al-15 after isothermally annealing at 400, 45
for the time periods ranging from 900 to 3687200 seconds.

T_p °C	ANNEALING TIME IN SECONDS										
	900	1800	3600	7200	14400	28800	57600	115200	230400	460800	921600
	HARDNESS HVN (5kg)										
400	121	119	113	113	110	109	110	105	105	103	92
	120	113	119	116	111	112	110	107	106	102	103
	118	113	120	114	120	109	111	107	106	103	106
	117	112	100	110	118	109	110	105	105	100	103
	MEAN HARDNESS HVN (5kg)										
	119	113	113	114	115	110	110	106	105	102	102
450	113	110	102	98	103	102	96	99	95	91	92
	113	111	107	104	103	102	102	100	97	89	92
	111	111	106	103	104	103	100	100	98	93	92
	109	110	108	105	102	102	100	98	96	93	91
	111	107	109	104	102	103	100	94	95	92	85
	MEAN HARDNESS HVN(5kg)										
	111	110	106	103	103	102	100	98	96	91	90
500	105	101	99	92	93	90	88	86	82	78	63
	102	103	101	94	93	90	88	86	83	78	80
	105	102	102	95	96	91	89	86	84	80	80
	106	102	99	95	96	91	89	86	84	80	80
	104	97	98	95	91	89	88	87	83	78	77
	MEAN HARDNESS HVN(5kg)										
	104	101	100	94	93	90	89	86	83	78	76
550	99	99	92	89	86	84	84	80	77	69	65
	101	97	93	89	87	84	84	79	79	76	75
	102	97	94	88	87	85	83	79	78	76	74
	102	98	92	88	87	85	83	80	79	75	74
	104	98	92	87	85	84	81	80	77	74	70
	MEAN HARDNESS HVN(5kg)										
	102	98	93	88	86	84	83	80	78	74	71

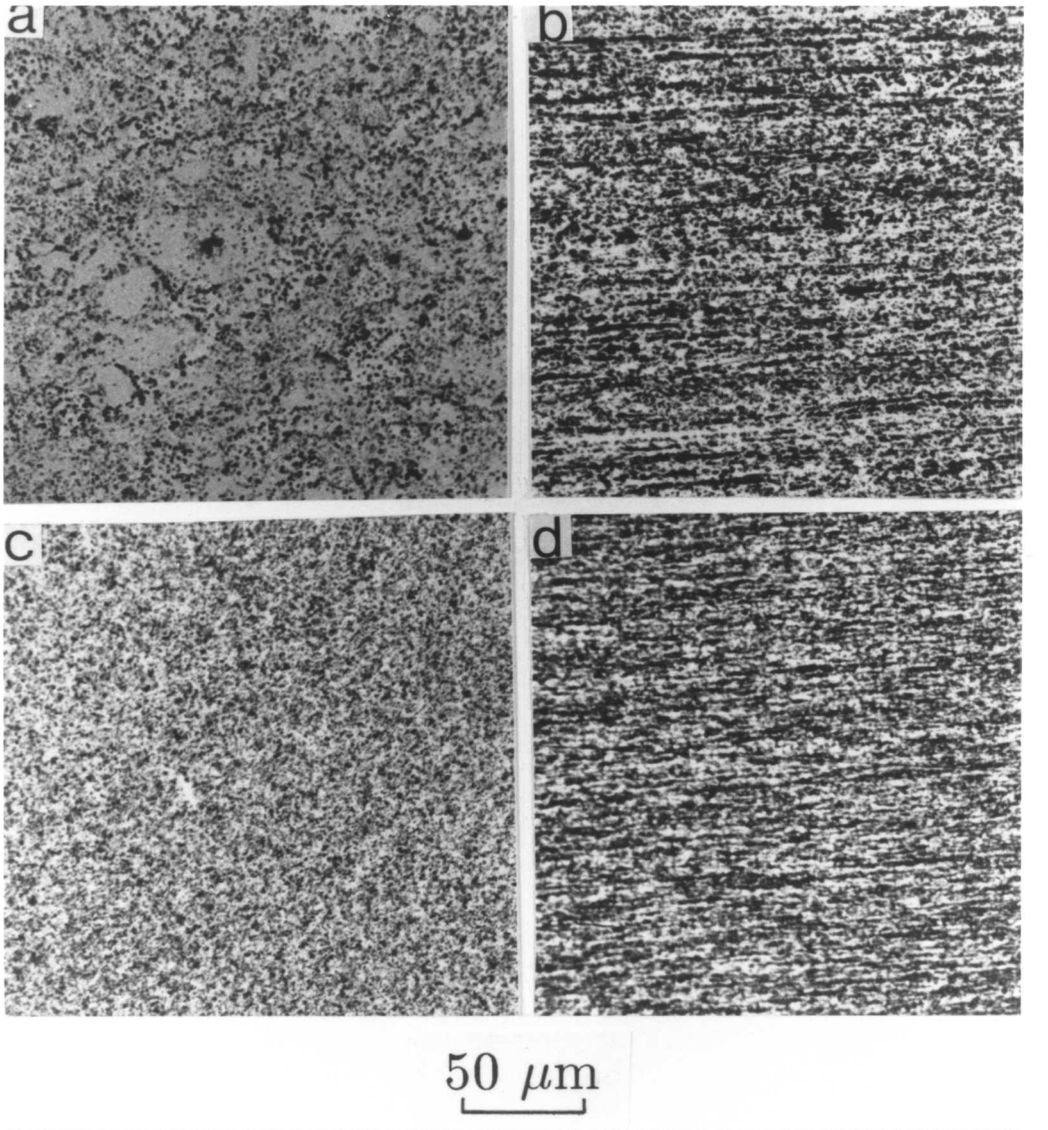

Figure 9.1. Optical micrographs showing the grain structure for aluminium alloys Al-5 and Al-15, in the as-received condition and after deformation.

a. Transverse section of alloy Al-5, in the as-received condition.

b. Longitudinal section of alloy Al-5, after deformation.

c. Transverse section of alloy Al-15, in the as-received condition.

d. Longitudinal section of alloy Al-15, after deformation.

Note the relatively large particle size and inhomogeneous distribution of particles in Al-5, when compared with Al-15.

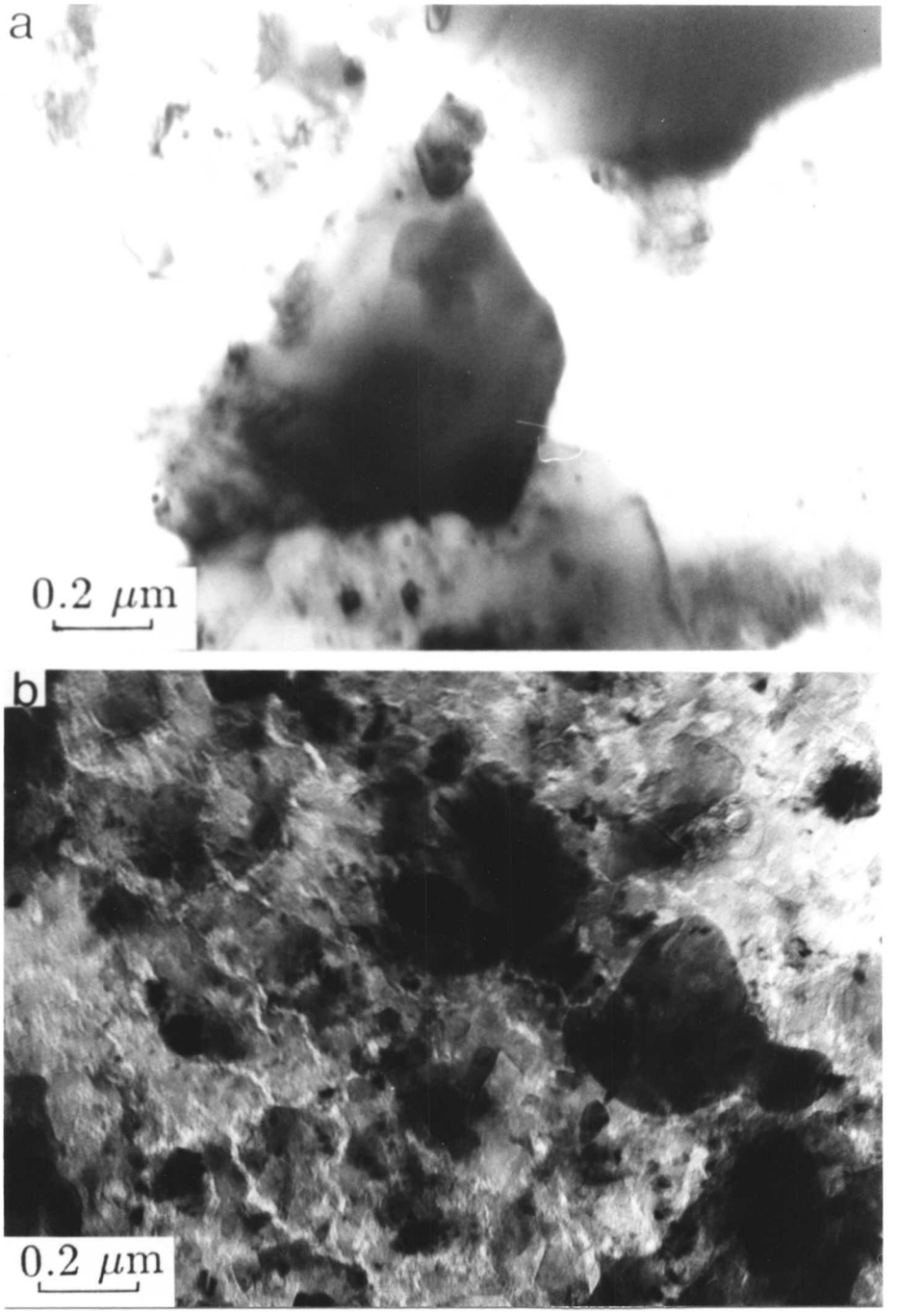

Figure 9.2. Transmission electron micrographs of rapidly solidified aluminium alloy Al-5.

a. Alloy Al-5, in the as-received condition, from the transverse section.

b. Alloy Al-5, after deformation, from the transverse section.

Note that the particles and phases, have not yet been characterised due to difficulties experienced during foil preparation, which are either because of the polishing solution used or the voltage applied.

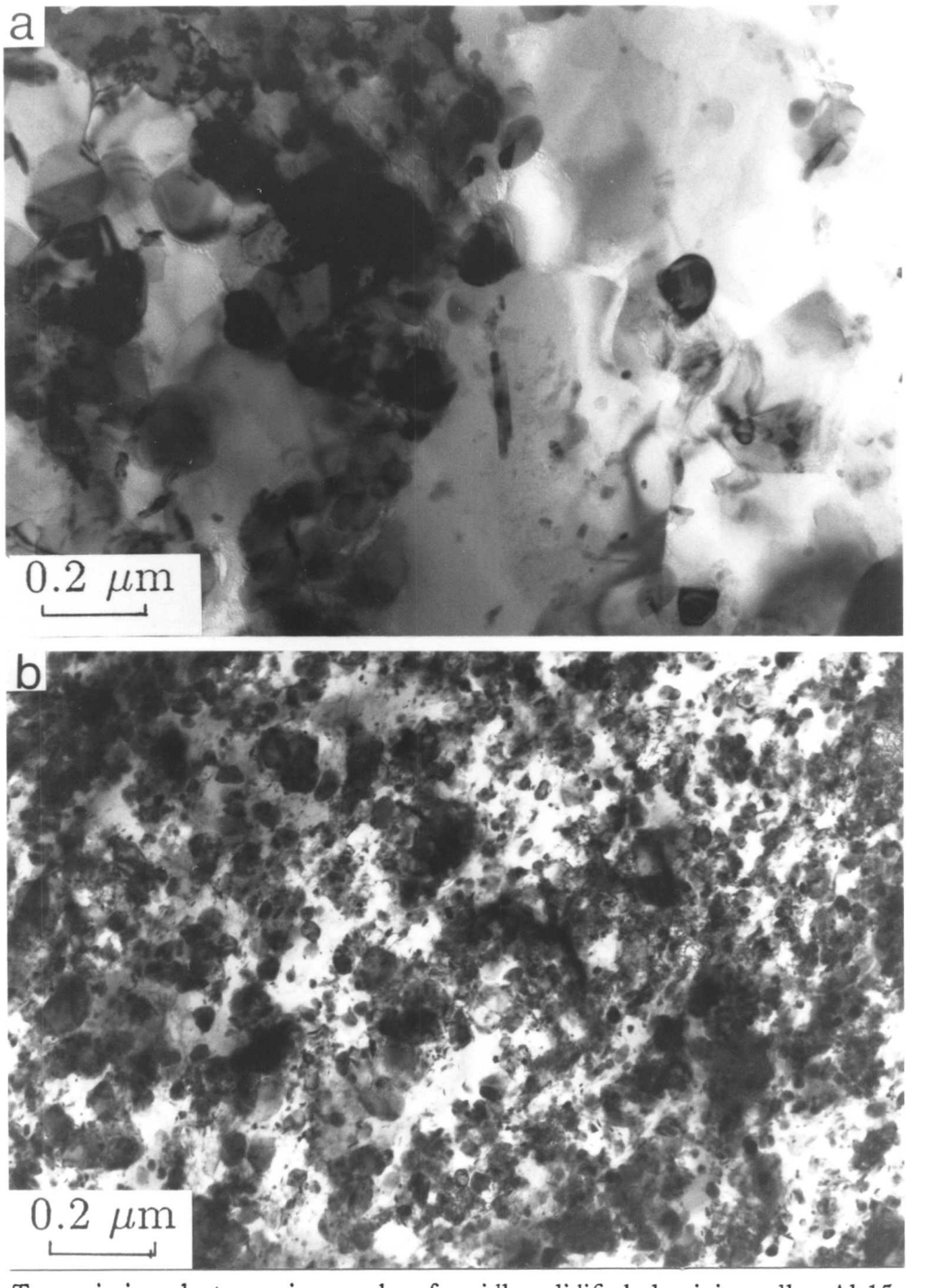

Figure 9.3. Transmission electron micrographs of rapidly solidified aluminium alloy Al-15.

a. Alloy Al-15, in the as-received condition, from the transverse section.

b. Alloy Al-15, after deformation, from the transverse section.

Note that the particles and phases, have not yet been characterised due to difficulties experienced during foil preparation, which are either because of polishing solution used, or the voltage applied.

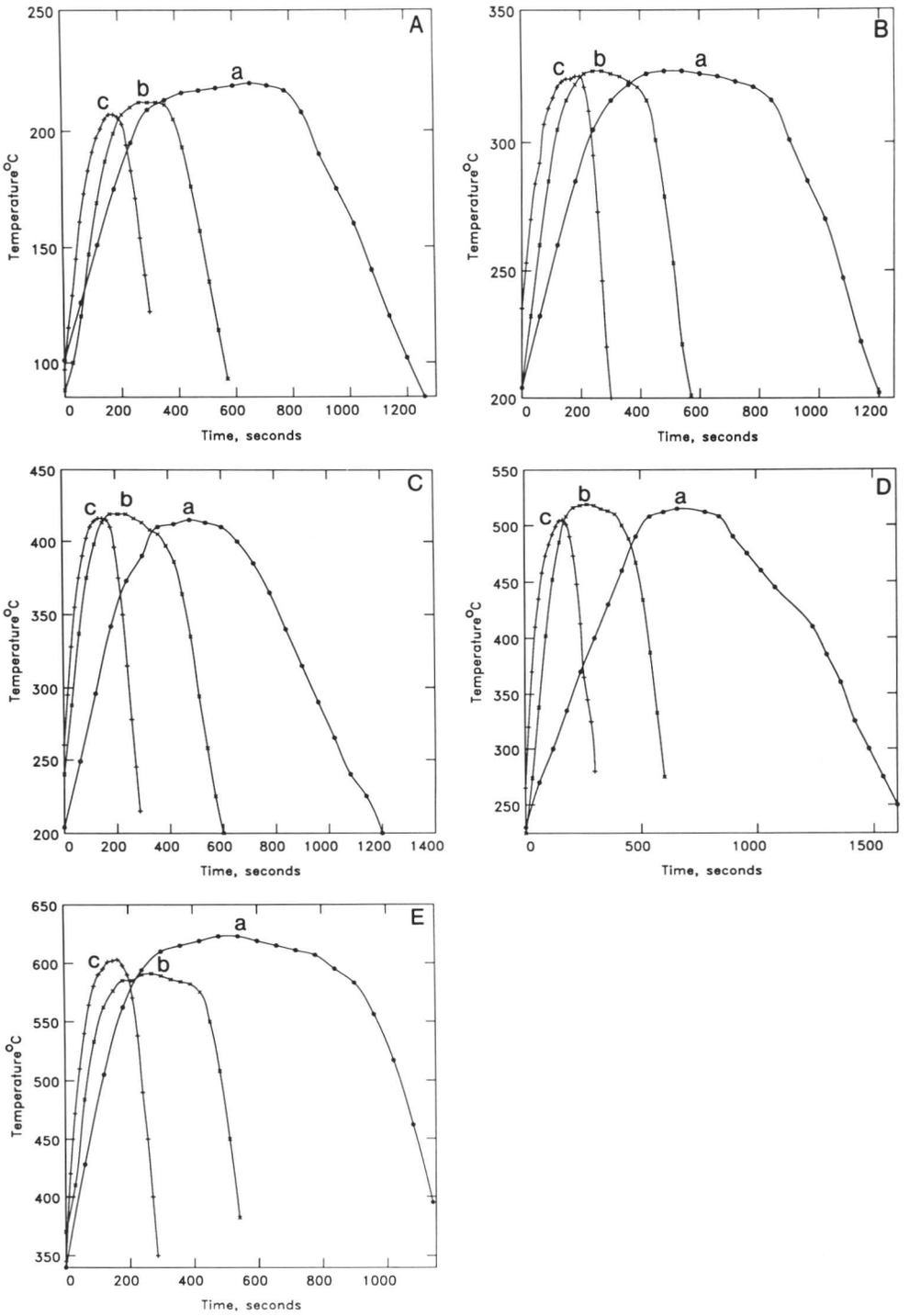

Figure 9.4. Temperature profiles recorded during zone annealing

Peak Temperature		Specimen Travel Speed
a. 200°C	c. 400°C	1.4 mm/min
b. 300°C	d. 500°C	3.2 mm/min
e. 600°C		5.0 mm/min

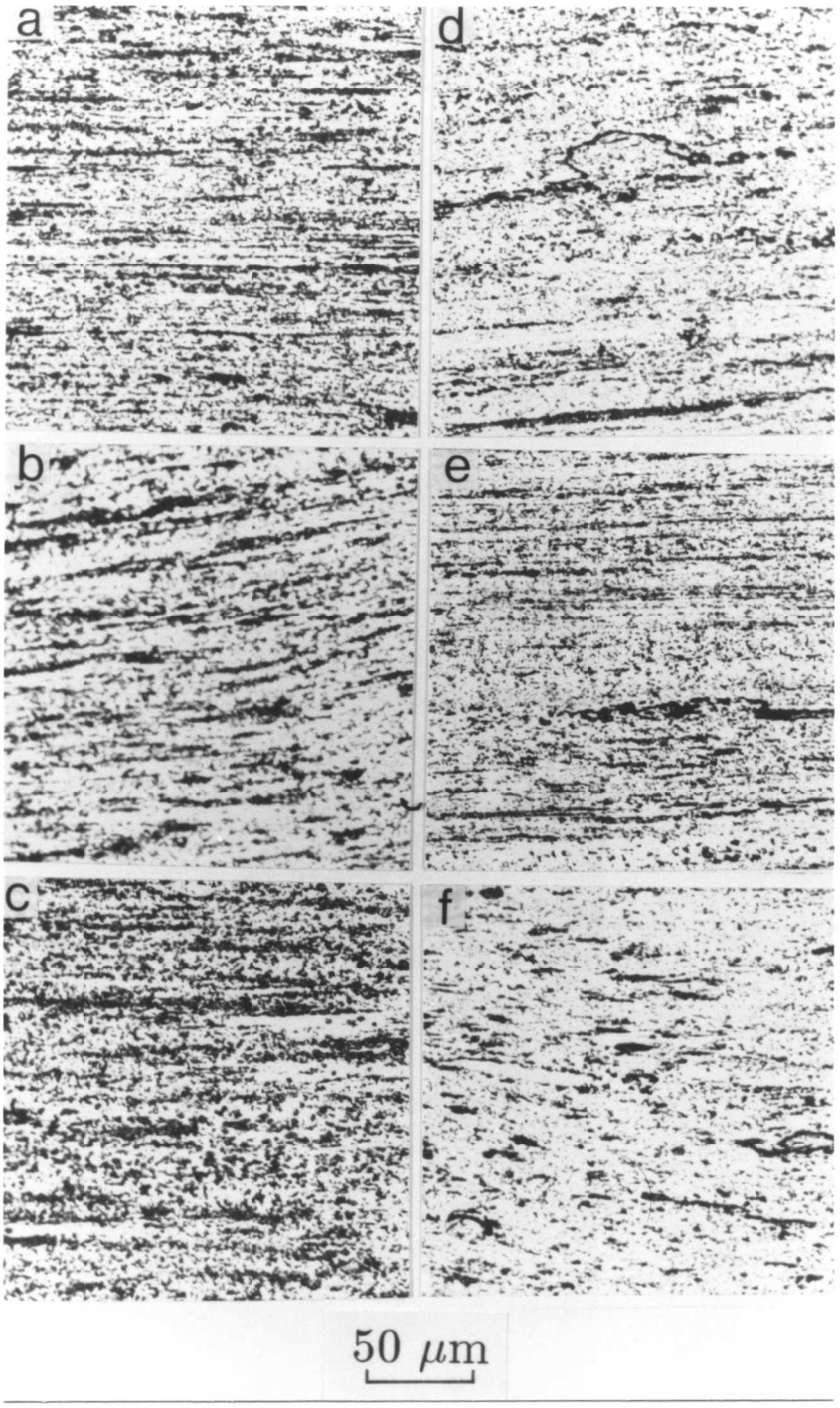

Figure 9.5. Optical micrographs recorded from longitudinal sections after zone annealing alloy Al-5 with T_p = 200 and 600°C, with different specimen travel speeds.

a. 1.4 mm/min T_p = 200°C, mean HV 106

b. 3.2 mm/min T_p = 200°C, mean HV 102

c. 5.0 mm/min T_p = 200°C, mean HV 102

d. 1.4 mm/min T_p = 600°C, mean HV 62

e. 3.2 mm/min T_p = 600°C, mean HV 71

f. 5.0 mm/min T_p = 600°C, mean HV 52

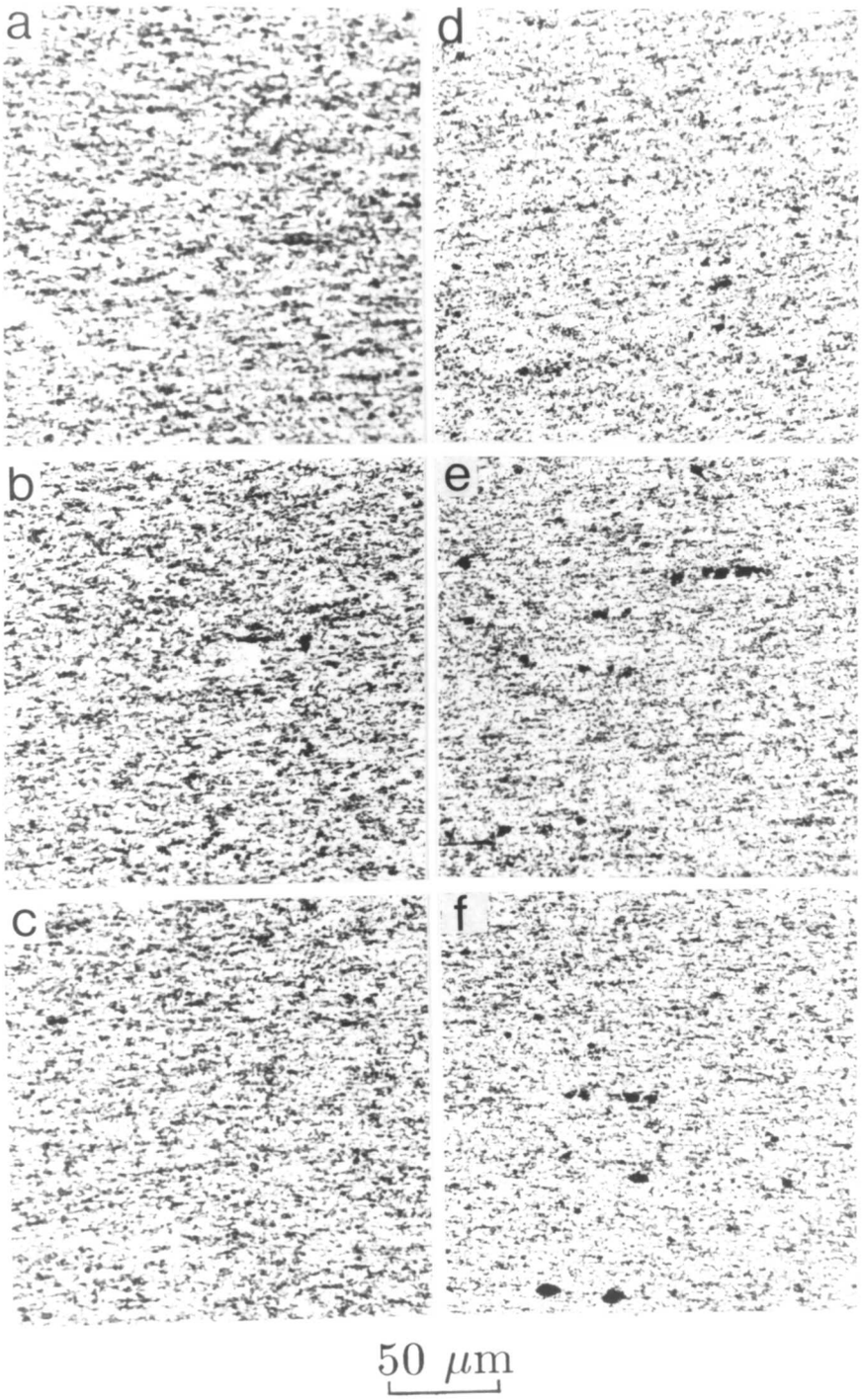

Figure 9.6. Optical micrographs recorded from longitudinal sections after zone annealing alloy Al-15 with T_p = 200 and 600°C, with different specimen travel speeds.

a. 1.4 mm/min T_p = 200°C, mean HV 108

b. 3.2 mm/min T_p = 200°C, mean HV 108

c. 5.0 mm/min T_p = 200°C, mean HV 105

d. 1.4 mm/min T_p = 600°C, mean HV 91

e. 3.2 mm/min T_p = 600°C, mean HV 91

f. 5.0 mm/min T_p = 600°C, mean HV 87

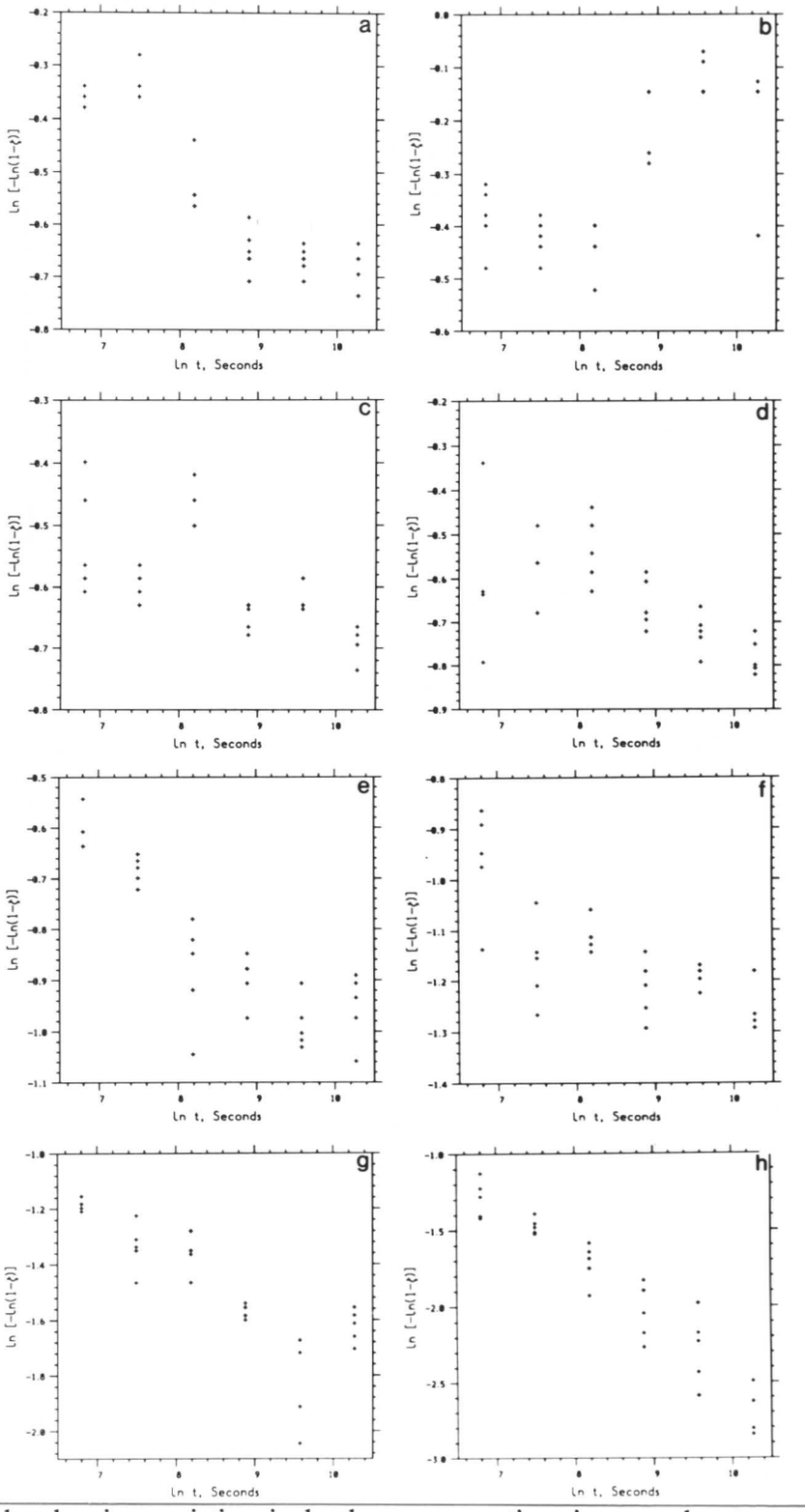

Figure 9.7. Graphs showing variation in hardness versus time in seconds, at temperatures ranging from 200 to 550°C for alloy Al-5.

a. 200°C b. 250°C c. 300°C

d. 350°C e. 400°C f. 450°C

g. 500°C h. 550°C

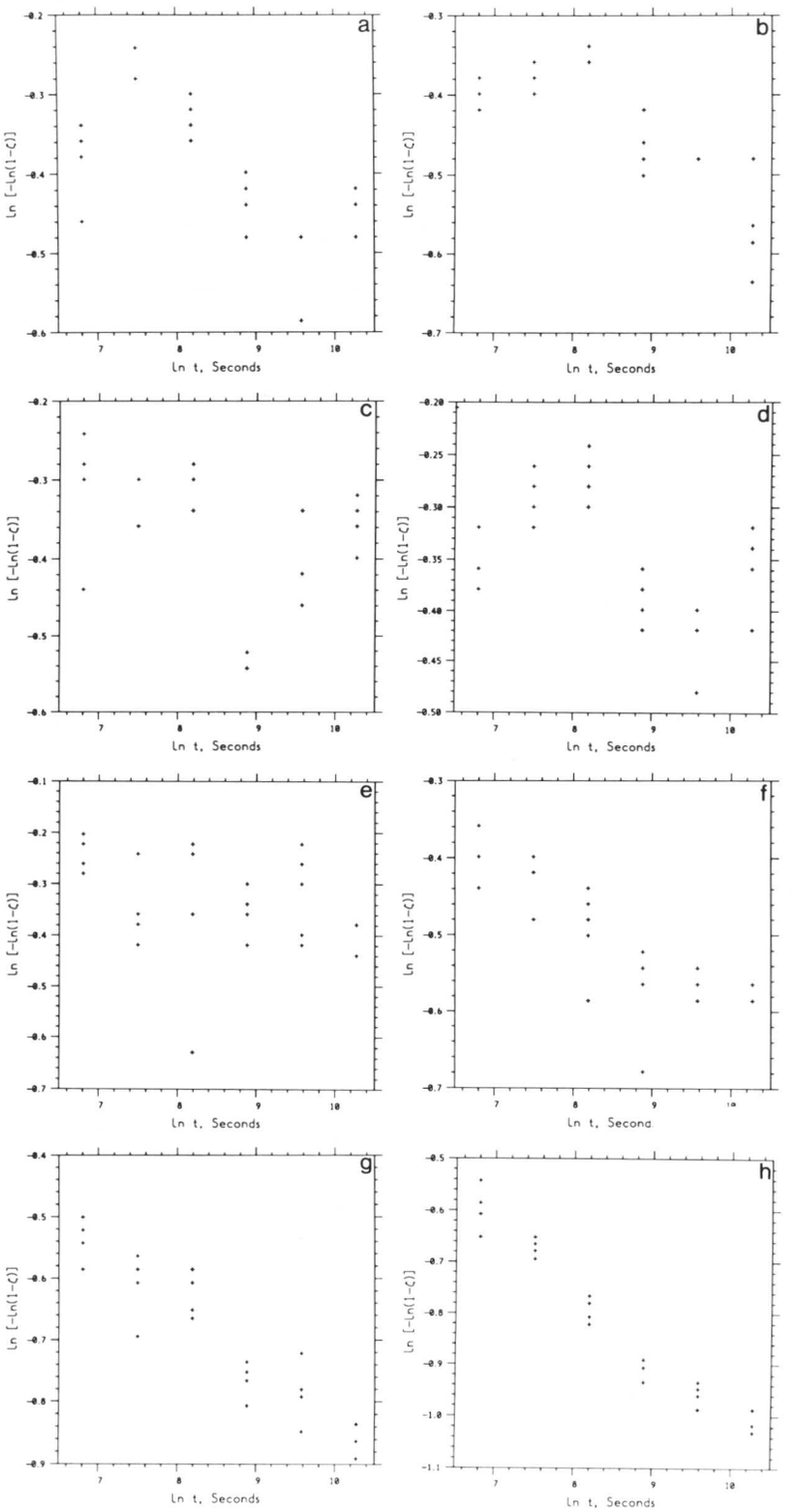

Figure 9.8. Graphs showing variation in hardness versus time in seconds, at temperatures ranging from 200 to 550°C for alloy Al-15.

a. 200°C b. 250°C c. 300°C

d. 350°C e. 400°C f. 450°C

g. 500°C h. 550°C

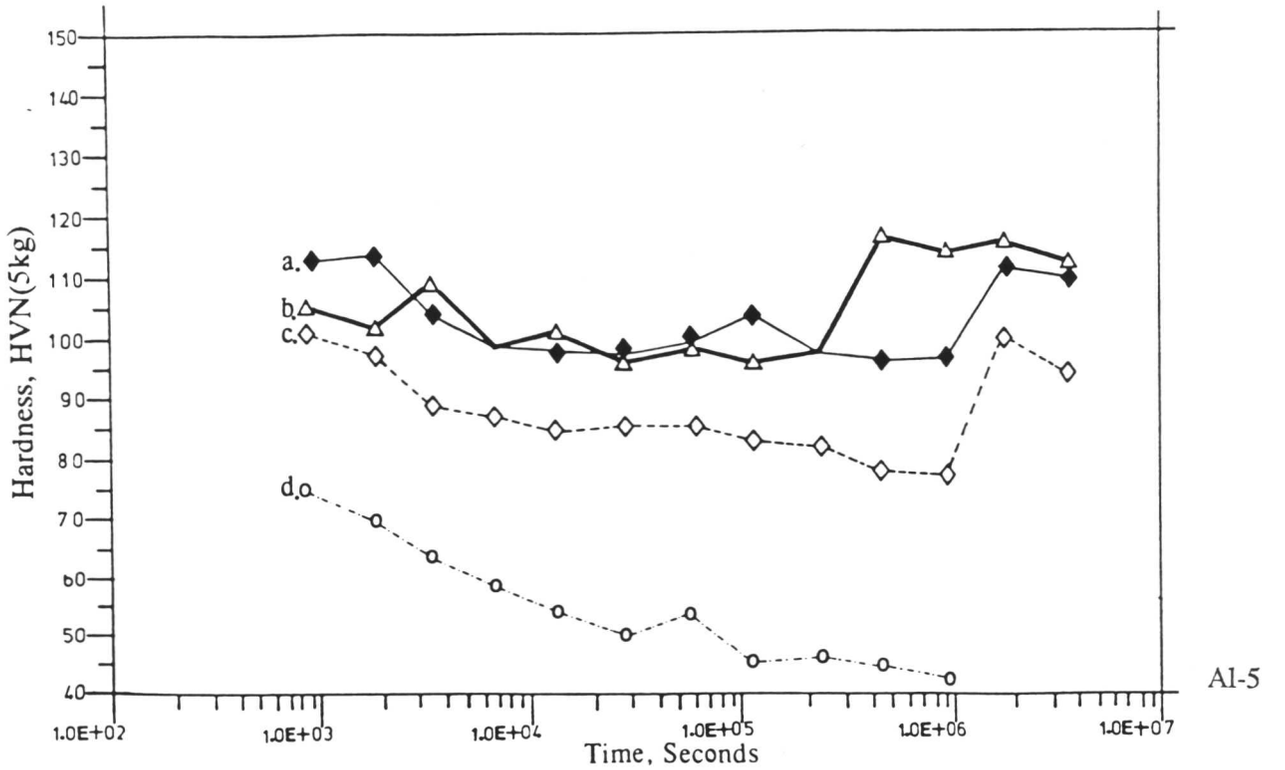

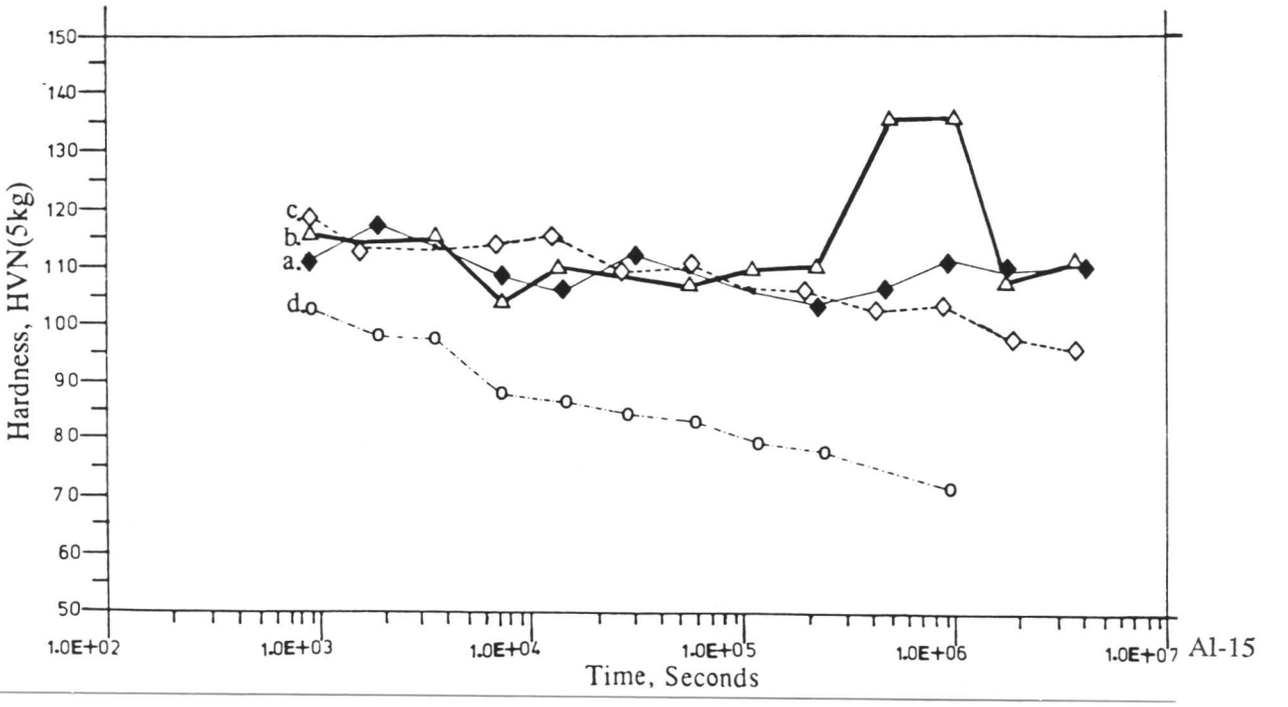

Figure 9.9. Graphs showing variation in hardness versus time in seconds, after isothermal annealing at:

a. 200°C b. 300°C c. 400°C d. 550°C

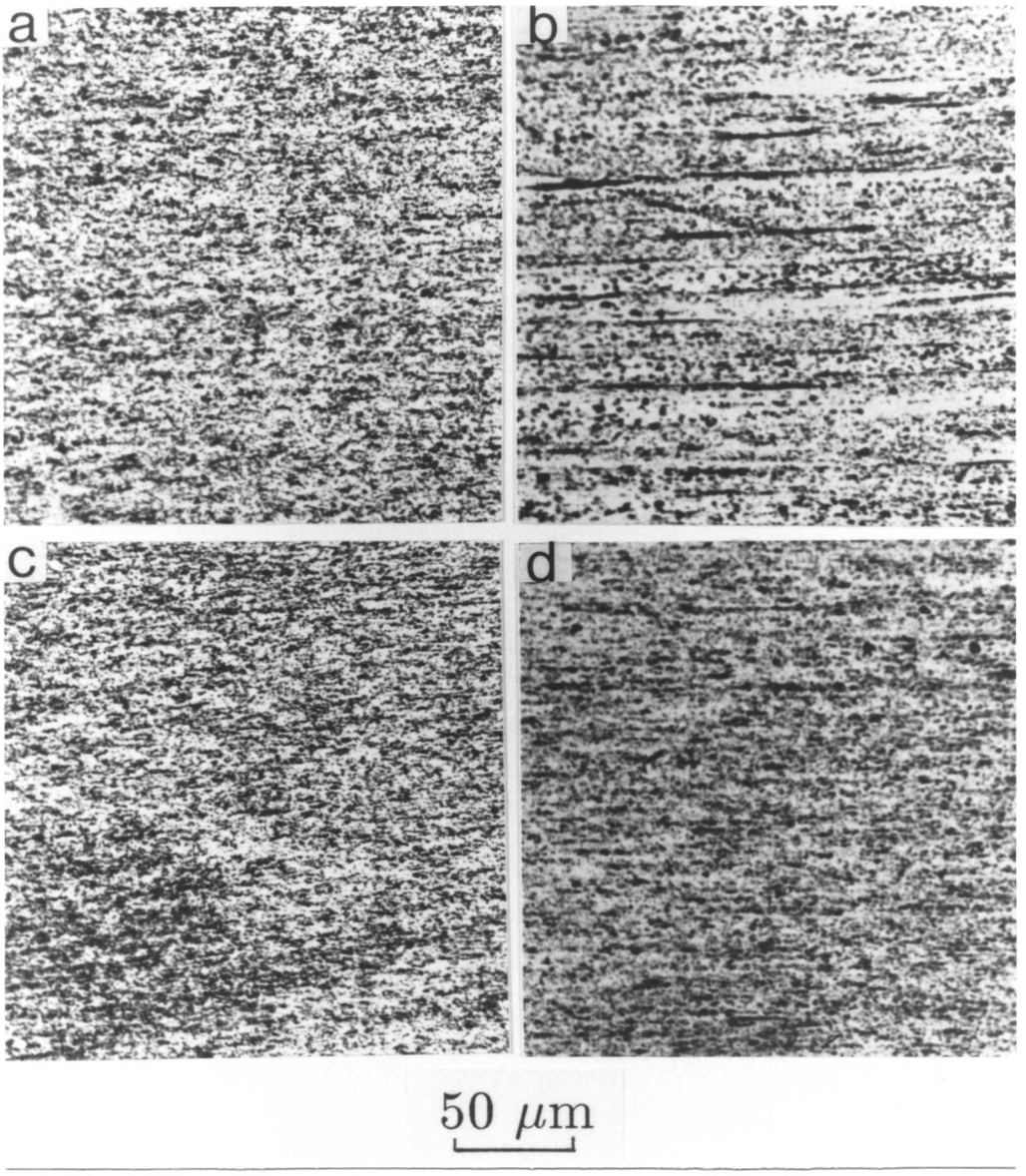

Figure 9.10. Optical micrographs showing the change in microstructure for the aluminium alloys Al-5 and Al-15, after isothermally annealing at 200°C for:

a. 900 s (Al-5),	mean HV 113
b 3687200 s (Al-5),	mean HV 110
c. 900 s (Al-15),	mean HV 112
d. 3687200 s (Al-15),	mean HV 110

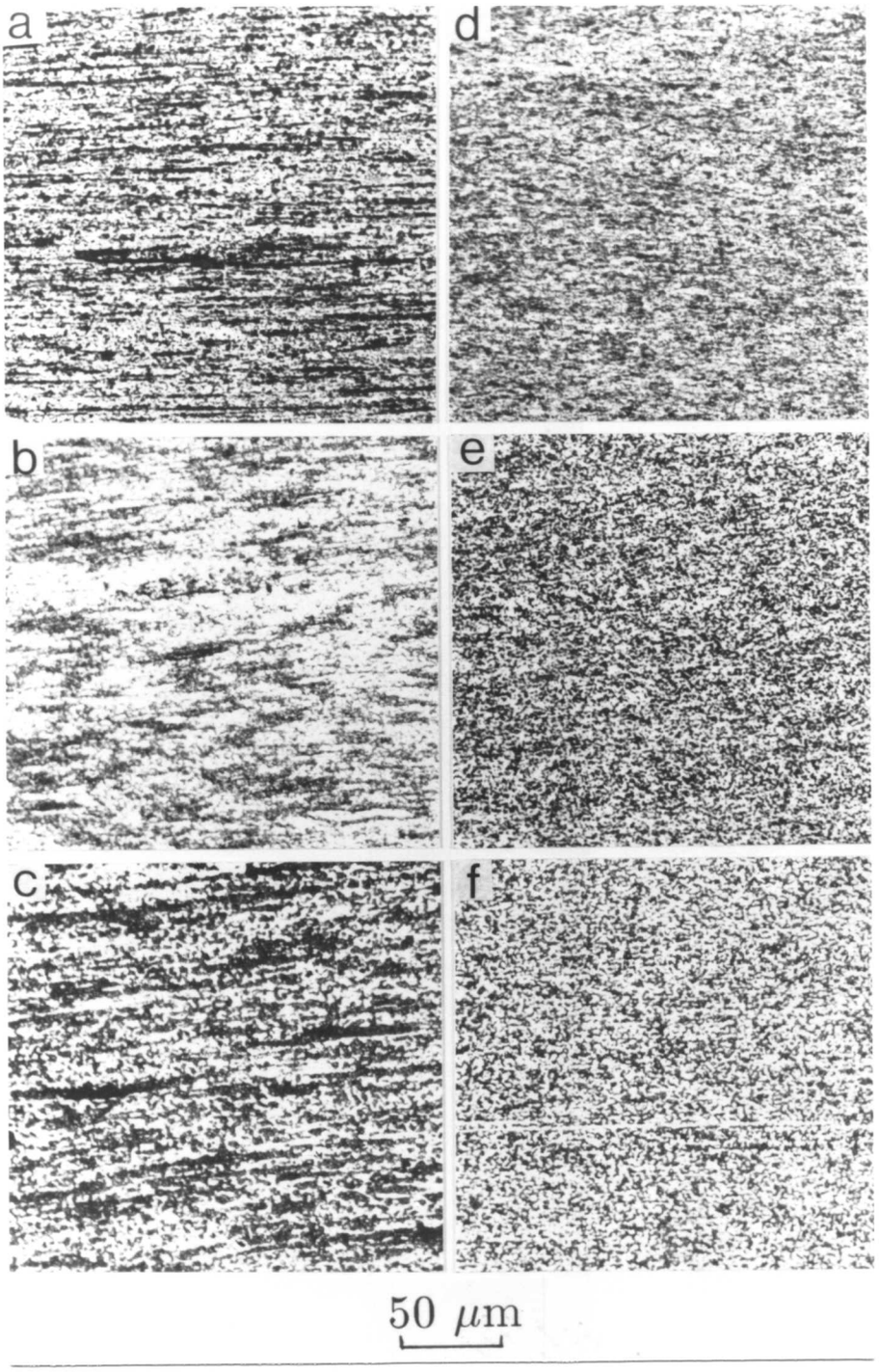

Figure 9.11. Optical micrographs showing the change in microstructure for the aluminium alloys Al-5 and Al-15, after isothermally annealing at 550°C for:

a. 900 s	(Al-5)	d. 900 s	(Al-15)
b. 115200 s	(Al-5)	e. 115200 s	(Al-15)
c. 921600 s	(Al-5)	f. 921600 s	(Al-15)

APPENDIX TWO

Zone Annealing Experiments Performed on Commercial Aluminium Alloys AA3003 and Al20

10.1 Introduction

In this appendix, the results obtained after zone annealing two different kinds of aluminium alloys designated AA3003 (Al-1.2Mn-0.7Fe-0.6Si-0.1Cu-0.1Zr wt%) and Al20 (Al-0.7Fe-1.25Cu-0.95Mg-0.1Zr-20SiC wt%) are discussed. These are both dispersion strengthened alloys.

10.2 Material

The aluminium alloy designated AA3003 was supplied by the Alcan International Ltd. Banbury Laboratory U.K., in the form of cold-rolled sheet. The cold rolling was carried out from 25 mm to approximately 3.5 mm (an 86% reduction). The aluminium alloy designated Al20 was supplied by British Petroleum. The production details for the both aluminium alloys are given in chapter 3.

Keeping in mind, the influence of working direction on directional recrystallisation as observed during zone annealing experiments on ODS nickel base superalloy (MA6000) and ODS ferritic steels (MA965 and MA957), it was thought convenient to prepare the specimens (4 x 20 mm) along the rolling direction. Most of the transmission electron and light optical microscopic studies performed on the longitudinal sections or in other words, on the sections parallel to the rolling direction.

Al20 was supplied in the form of bar, with the dimensions of 15 mm diameter and 1000 mm long. It was cold-swaged down to 7.50 mm diameter rod (~ 52% reduction) at ambient temperature. After cold-working specimens were finally cut to a length of 20 mm, using a slitting disc. Since the alloy AA3003 was supplied in the cold-rolled condition possessing a hardness value of 67 HVN(5kg), therefore no further deformation was applied. The hardness measurements were made in the as-received condition and after deformation on Al-20 were turned out as 57 and 70 HVN(5kg) respectively. The measured hardness values indicate that the amount of deformation applied to both the aluminium alloys AA3003 and Al20, has not significantly increased the hardness of these alloys.

10.3 AA3003 - Zone Annealing Experiments

Optical and transmission electron microscopy (figure 10.1-2) showed the expected elongated grain structure with a very low dislocation density. The particles were found randomly distributed in the matrix. The observations suggest that the material underwent dynamic recovery during the rolling operation.

The hardness from zone annealed samples are listed in Table 10.1a and the optical micrographs are shown in figure 10.3-5. An equiaxed grain structure was observed irrespective of the zone annealing conditions applied. The hardness results measured after each successful zone annealing experiments at the temperatures, are consistent with the microstructural observations. From Table 10.1a, it can be seen that the increase in temperature from 430 to 630°C, has not affected the microstructure at all.

The transmission electron microscopic studies revealed the effect of particles on the recrystallisation behaviour of aluminium alloy AA3003. Figure 10.6 taken from a thin foil prepared from the longitudinal section of the sample zone annealed at 430°C with a specimen travel speed of 0.2 mm/min., the figure shows the advancement of grain "A" towards grain "B" has been clearly stopped by the particle on the interface between both the grains. Another example of the particle pinning on the grain boundary is shown in figure 10.7. It is presumably the pinning effect which prevents a directional microstructure.

10.4 Results Obtained After Zone Annealing Aluminium Alloy Al20

The microstructure observed prior to and after deformation is shown in figure 10.9. and the corresponding hardness data are tabulated in Table 10.1b.

Optical micrographs shown in figures 10.10-12 reveal the microstructure of alloy Al20, after zone annealing at 430, 500 and 630°C respectively, with a range of specimen travel speeds (0.8, 1.4, 3.2 and 5.0 mm/min). Any changes in grain structure are not obvious due to the very high volume fraction of particles

10.5 Summary

After zone annealing, alloy AA3003 exhibited equiaxed microstructure, even when heat treated at relatively higher temperature (630°C). A significant decrease in hardness was measured after annealing at the range of temperatures suggesting a softening due to recrystallisation. From the

transmission electron microscopic studies, particles were found to pin the advancing grain boundaries, which could be a reason for the lack of directional grain growth during zone annealing.

After zone annealing, alloy Al20 exhibited considerable influence of deformed structure and high hardness values at a range of temperatures. From the microstructural observations and hardness data obtained after annealing alloy Al20, it can be said that due to higher volume fraction of SiC particles, the material cannot be easily recrystallised.

Table 10.1a. Microstructure and Vickers hardness data obtained for Alloy AA3003, after zone-annealing at 430, and 630 °C with different specimen travel speeds. HV in the as-receieved condition was 67 HVN(5

Tp °C	Specimen Condition	Specimen Travel speed mm/min								Hardness Vickers HVN(5kg)								M
		0.2	0.4	0.8	1.4	3.2	5.0	7.7	10.0	0.2	0.4	0.8	1.4	3.2	5.0	7.7	10.0	0.2
430	Pl: RD	X	X	X	X	X	X	X	X	32	32	31	32	33	32	33	32	32
										32	31	32	32	33	32	33	32	
										32	31	32	31	32	32	33	32	
										32	31	31	32	34	32	33	33	
										31	31	32	32	32	32	32	33	
500	Pl: RD	X	X	X	X	X	X	X	X	31	31	31	31	33	32	32	32	31
										31	31	31	31	33	32	32	32	
										31	31	30	31	31	33	32	32	
										30	31	31	31	32	32	32	32	
										30	31	31	31	32	31	32	32	
630	Pl: RD	X	X	X	X	X	X	X	X	31	31	31	32	32	34	33	32	31
										31	31	31	32	32	33	33	31	
										32	31	31	32	32	34	34	32	
										31	32	31	32	32	33	34	32	
										31	32	31	32	32	33	34	32	

Table 10.1b. Microstructure and Vickers hardness data obtained for aluminium alloy desginated as Al-20, af
430, 500 and 630 ^{0}C with different specimen travel speeds. Hardnesses measured in the as-rec
deformation (an 50% reduction by cold-swaging) were 57 and 70 HVN(5kg) respectively.

T_P ^{o}C	Specimen	Specimen Travel Speed mm/min				Hardness Vickers HVN(5kg)				Mean
	Condition	0.8	1.4	3.2	5.0	0.8	1.4	3.2	5.0	0.8
430	PI: SD	D	D	D	D	60	57	62	61	58
						58	58	58	61	
						57	59	57	59	
						58	58	59	60	
						56	58	60	59	
500	PI: SD	D	D	D	D	58	60	61	58	58
						59	61	62	58	
						57	59	61	57	
						58	59	61	58	
						56	58	61	56	
630	PI: SD	D	D	D	D	59	63	60	60	58
						57	60	58	59	
						59	62	59	59	
						58	62	61	59	
						59	62	58	58	

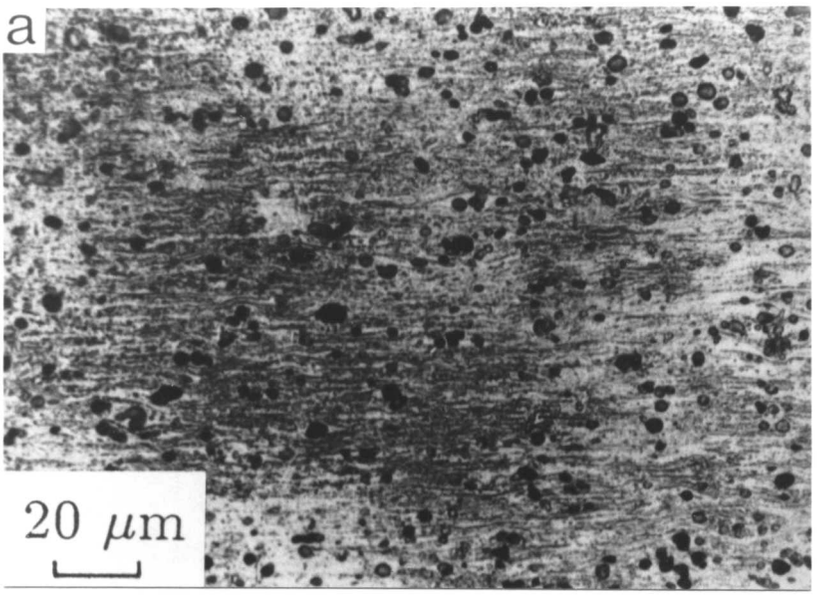

Figure 10.1. The as-received optical microstructure of alloy AA3003.

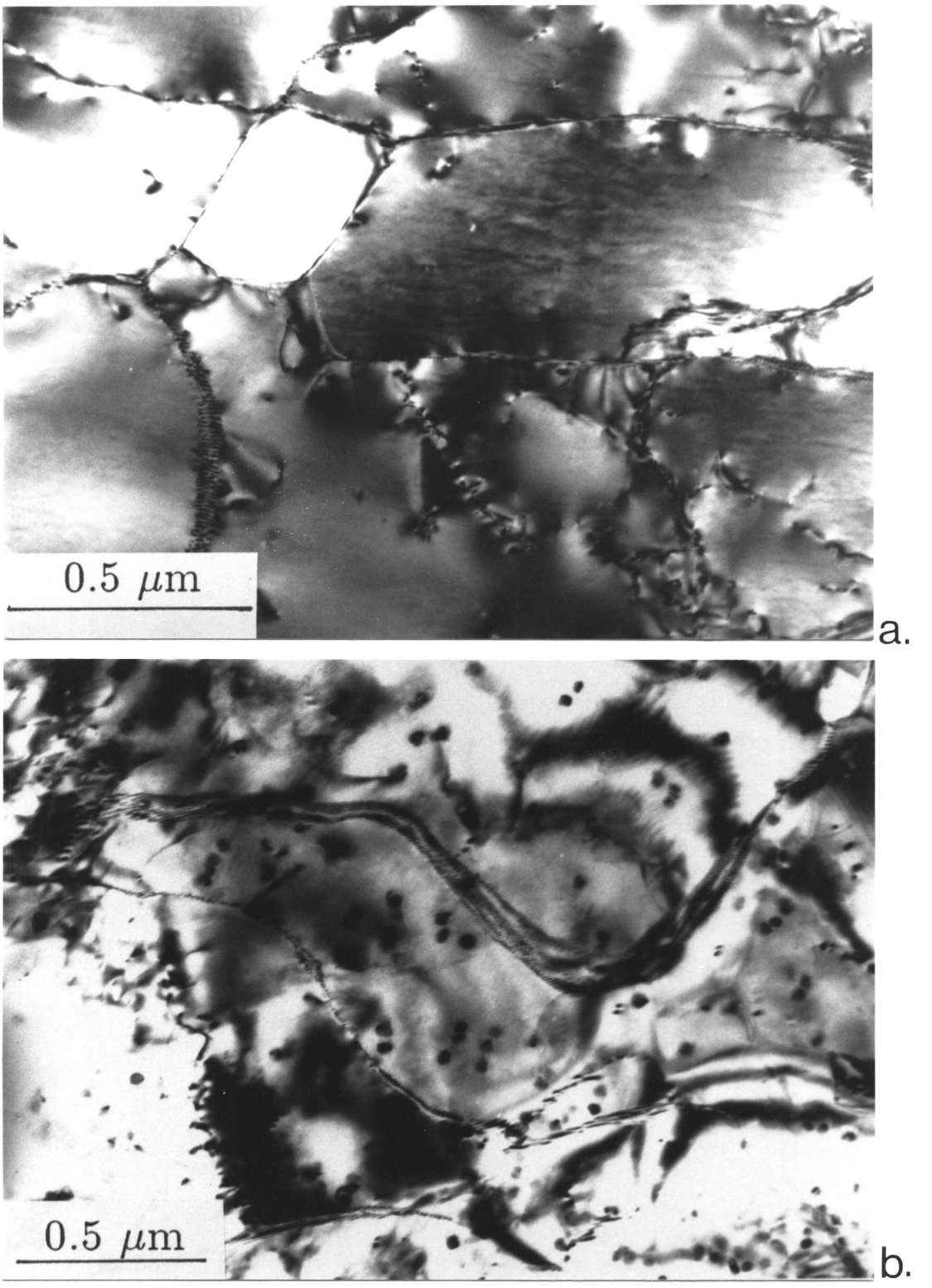

Figure 10.2. Transmission electron micrographs showing the microstructure of alloy AA3003 in the as-received condition.

a. Represents the microstructure observed on a transverse section of sheet.

b. Represents the microstructure observed on a longitudinal section.

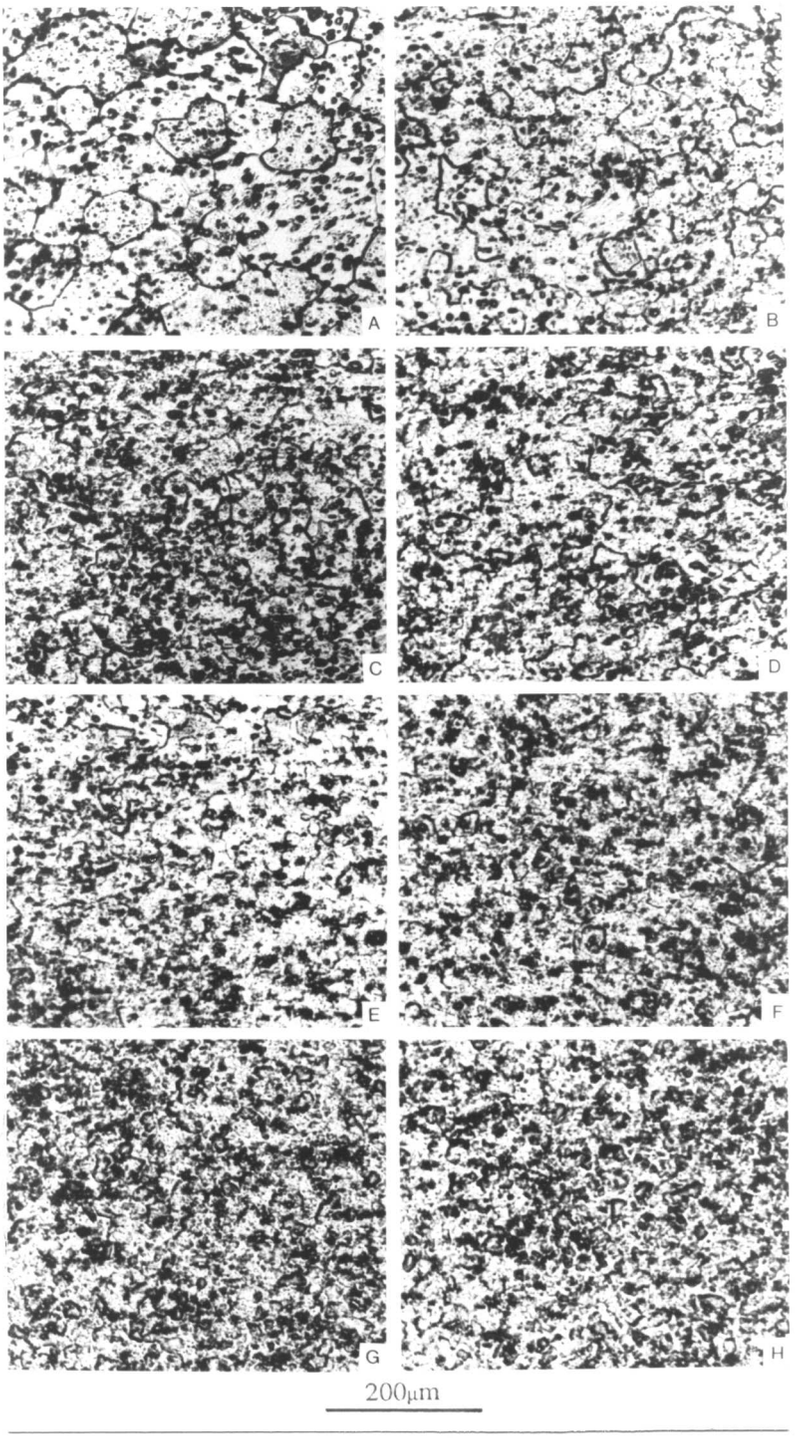

Figure 10.3 Optical micrographs showing the equiaxed grain structure observed after zone annealing alloy AA3003 at 430°C with following specimen travel speeds (mm/min):

A. 0.2 B. 0.4 C. 0.8 D. 1.4

E. 3.2 F. 5.0 G. 7.7 H. 10.0

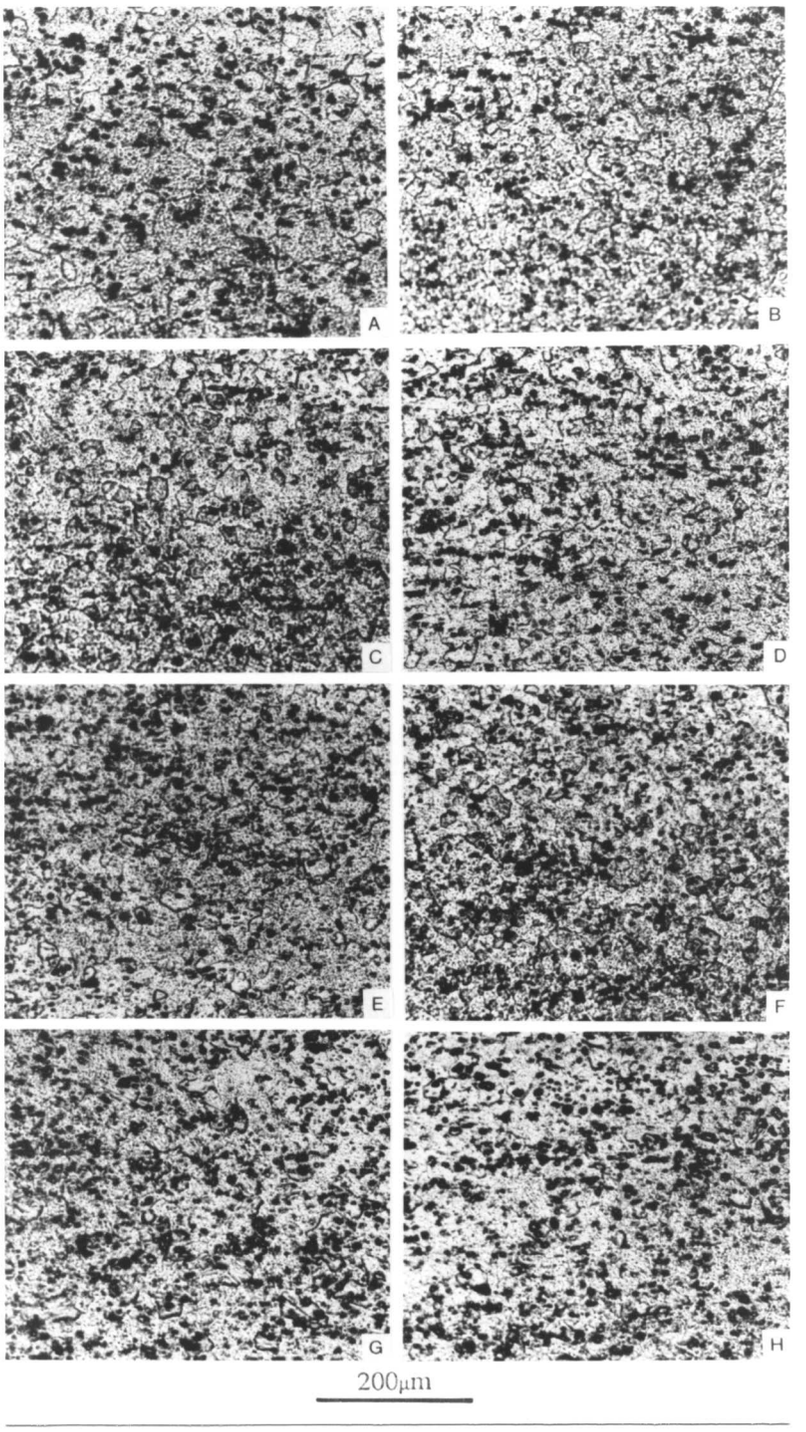

Figure 10.4. Optical micrographs taken after zone annealing alloy AA3003 at 500°C with following specimen travel speeds (mm/min):

A. 0.2	B. 0.4	C. 0.8	D. 1.4
E. 3.2	F. 5.0	G. 7.7	H. 10.0

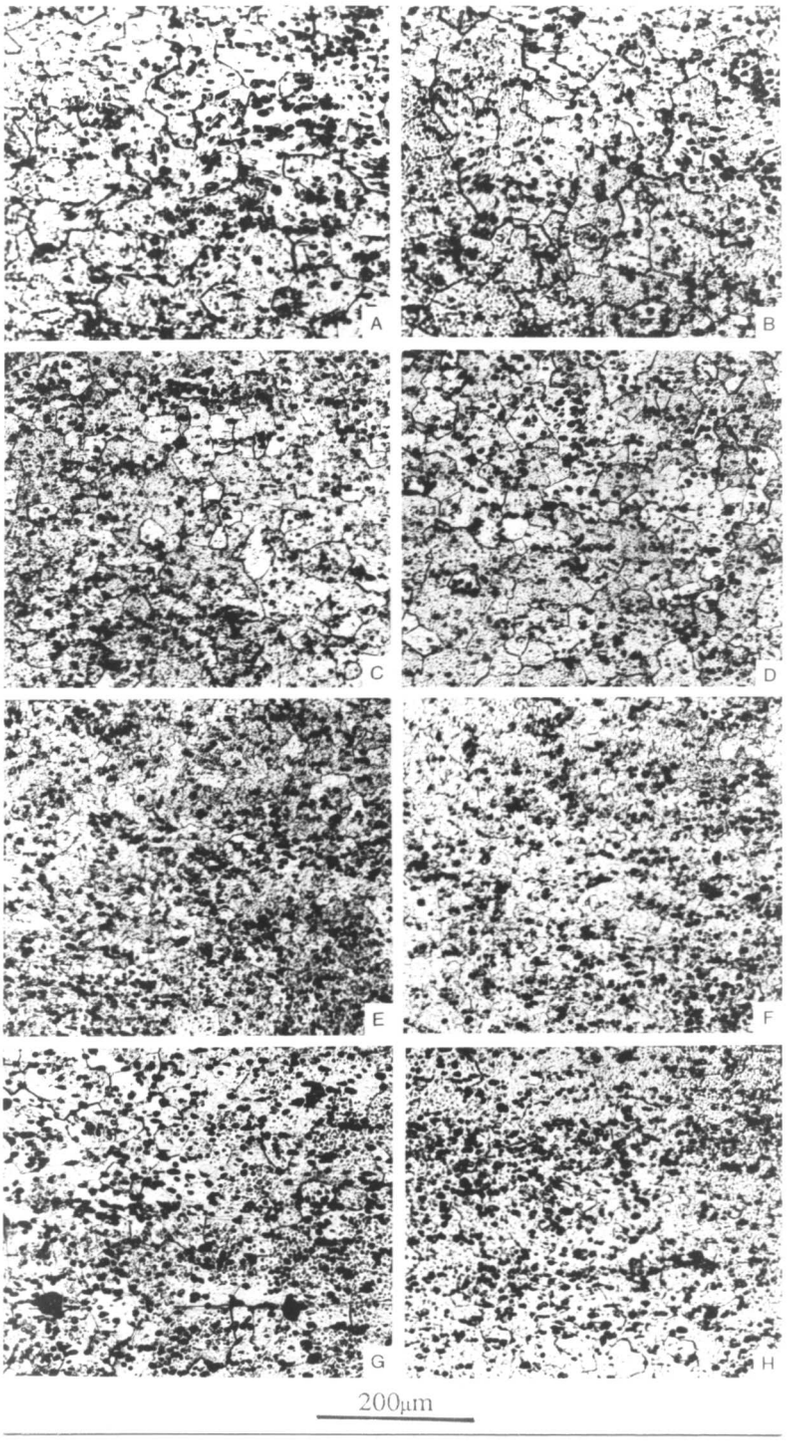

Figure 10.5. Optical micrographs shows the equiaxed grain structure observed after zone annealing alloy AA3003 at 630°C with following specimen travel speeds (mm/min):

A. 0.2 B. 0.4 C. 0.8 D. 1.4

E. 3.2 F. 5.0 G. 7.7 H. 10.0

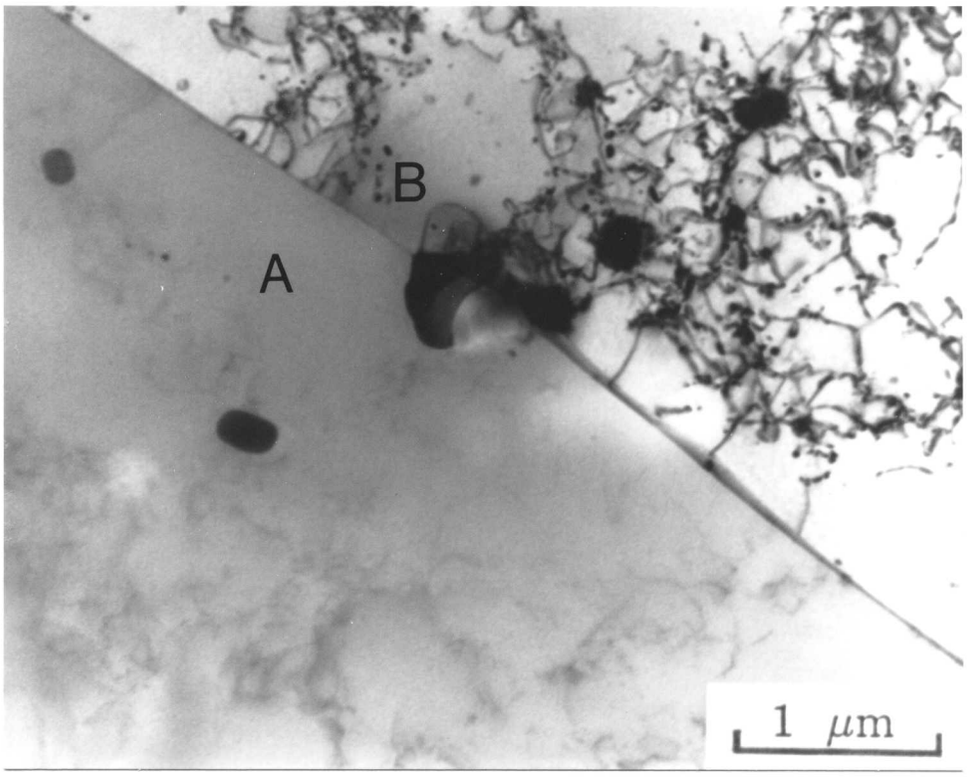

Figure 10.6. Retardation of the advancement of grain "A" towards grain "B" by the particle pinning on the interface (Z.A @ 430°C / 0.2 mm/min).

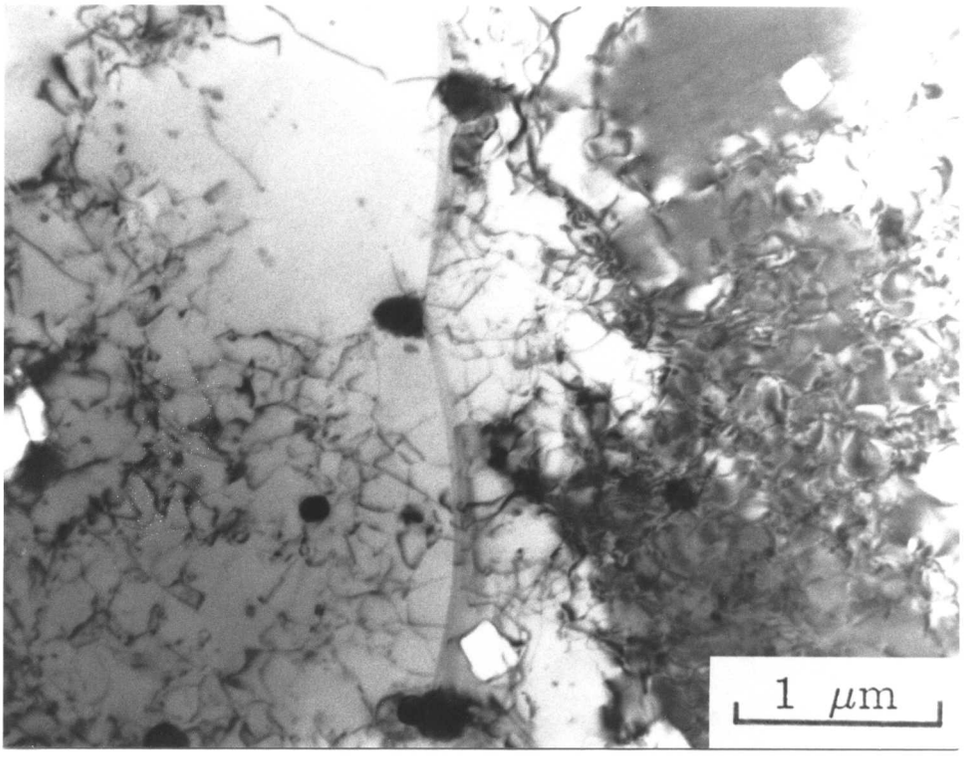

Figure 10.7. Electron micrographs illustrates the pinning effect (Z.A @ 430°C / 0.2 mm/min).

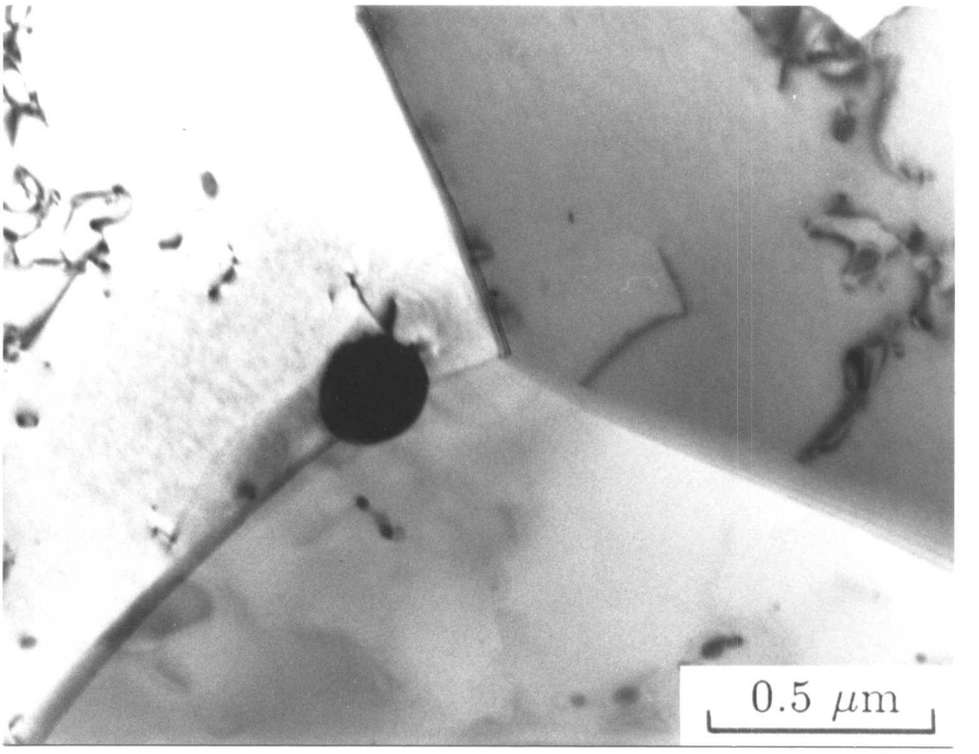

Figure 10.8. Transmission electron micrograph shows a typical recrystallised region from the sample zone annealed at 430°C with a specimen travel speed of 0.2 mm/min.

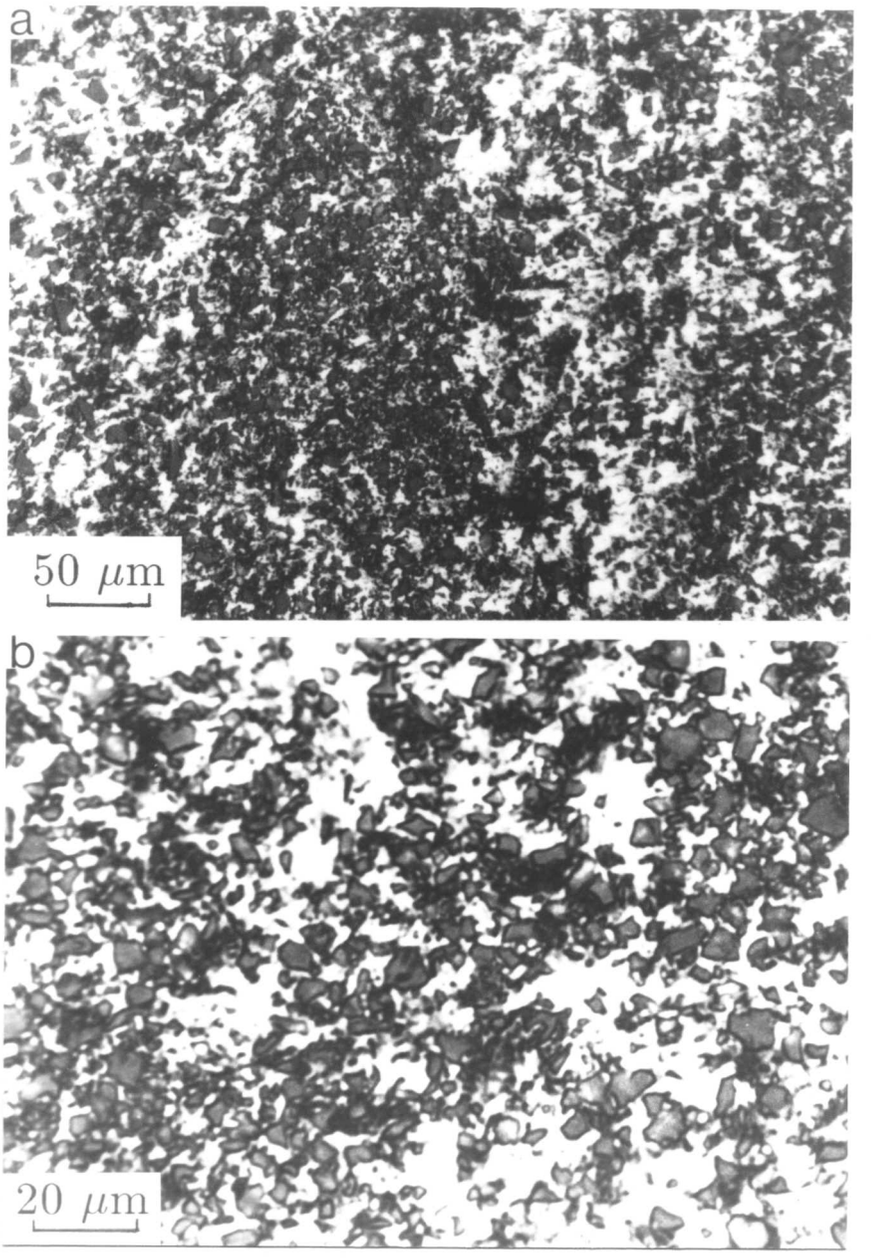

Figure 10.9. Optical micrographs recorded for alloy Al20, shows the microstructure of the alloy prior to and after deformation.

a) After deformation

b) As-received condition.

Note the relatively large particle size and inhomogeneous distribution of particles, when compared with AA3003.

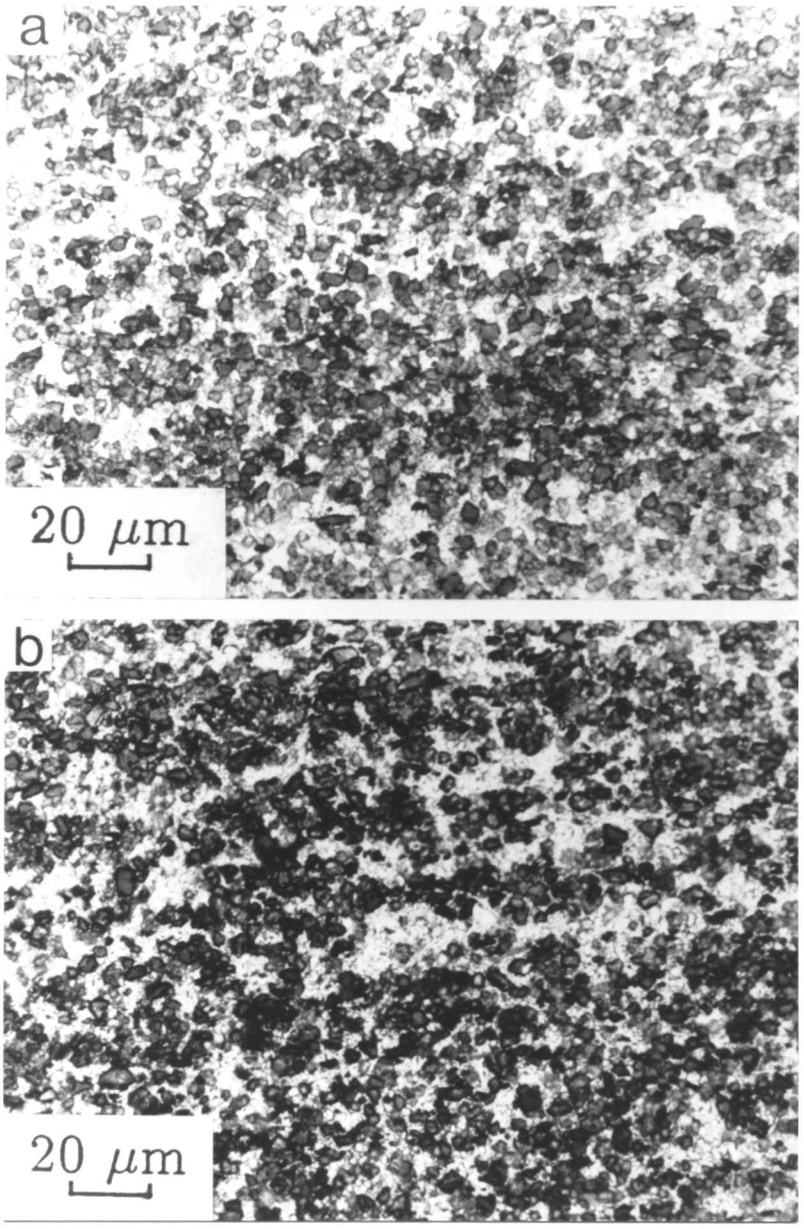

Figure 10.10. Optical micrographs taken after zone annealing the samples of alloy Al20

a) Z.A @ 430°C/ 0.8 mm/min.

b) Z.A @ 430°C/ 5.0 mm/min.

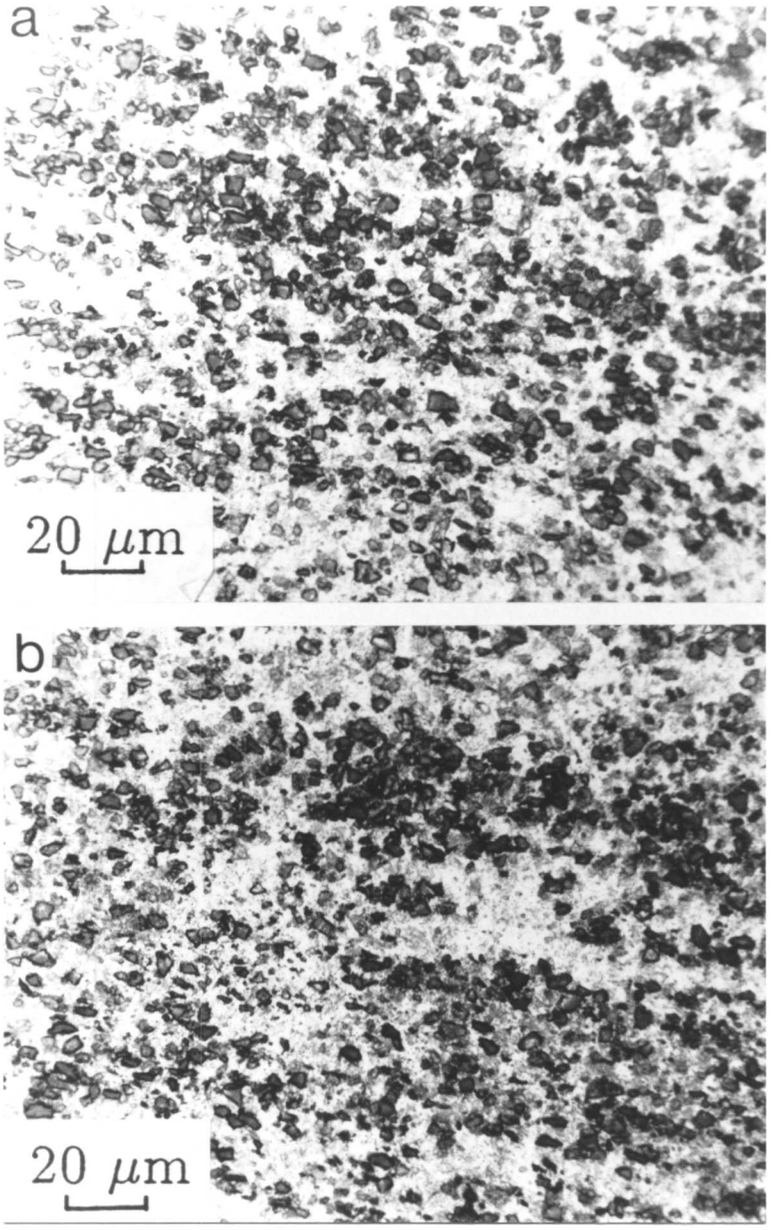

Figure 10.11. Optical micrographs showing the microstructure of alloy Al20 after zone annealing at 500°C with specimen travel speeds of (a) 0.8 mm/min and (b) 5.0 mm/min.

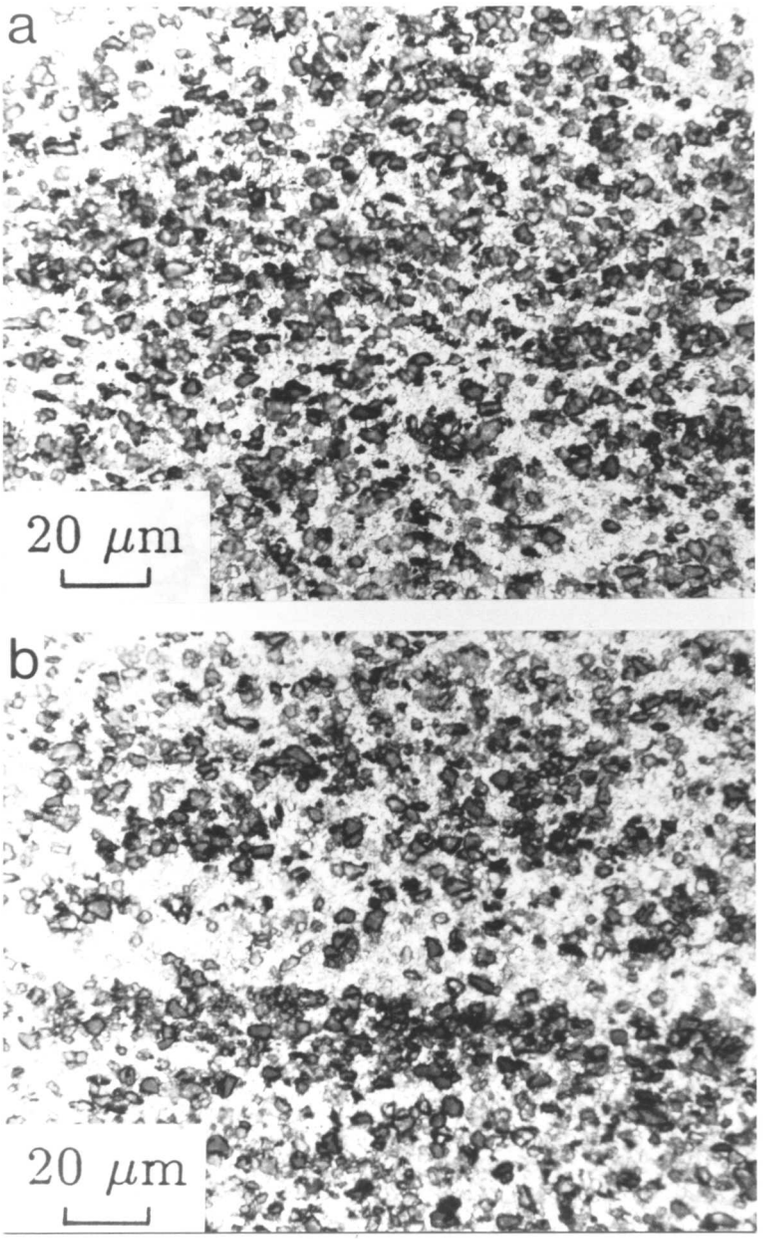

Figure 10.12. Light optical micrographs recorded from the samples zone annealed at 630°C. Note the significant influence of deformed structure even after zone annealing at relatively higher temperature.

a) Z.A @ 630°C/ 0.8 mm/min.

b) Z.A @ 630°C/ 5.0 mm/min.

APPENDIX THREE

```
C ***********************************************************************
C PROGRAM TO CALCULATE THE ACTIVATION ENERGY Q USING THE CONCEPT
  OF KINETIC STRENGTH OF AN ANISOTHERMAL HEAT TREATMENT
C ***********************************************************************
   IMPLICIT REAL*8 (A-H,K-Z)
   DOUBLE PRECISION TE(2), X1(200),Y1(200),X2(200),Y2(200)
   READ(5,*) I1
   DO 10 I=1,I1
   READ (5, *) X1(I),Y1(I)
10 CONTINUE
   READ (5, *) I2
   DO 20 I=1,I2
   READ (5, *) X2(I),Y2(I)
20 CONTINUE
   ACC=1.0D-5
   Q1=257500.0D+00
   Q2=Q1*1.00001D+00
100 CALL SUB1 (Q1,T1,I1,X1,Y1)
       CALL SUB1 (Q1,T2,I2,X2,Y2)
   TE(1)=T1
   TE(2)=T2
   F1=FUN(Q1,TE)
   CALL SUB1 (Q2,T1,I1,X1,Y1)
   CALL SUB1 (Q2,T2,I2,X2,Y2)
   TE(1)=T1
   TE(2)=T2
   F2=FUN(Q2,TE)
```

```
      IF(DABS(F2) .LT. ACC) GOTO 300
      NEW=Q2-F2/(F2-F1)*(Q2-Q1)
      WRITE(6,*) 'F1,F2,Q=',F1,F2,NEW
      Q1=Q2
      Q2=NEW
      GOTO 100
300   WRITE(6,99) Q2,F2
99    FORMAT(1H ,'Q-VALUE=',D16.8,' ACC=',D12.4)
      STOP
      END
C ******************************************************************************
      SUBROUTINE SUB1(Q,T,II,X,Y)
      IMPLICIT REAL*8(A-H,K-Z)
      DOUBLE PRECISION X(200),Y(200),A(200)
      EXTERNAL D01GAF
      DO 10 I=1,II
      A(I)=EXP(-Q/(8.3143D+00*(Y(I)+273.0D+00)))
10    CONTINUE
      IFAIL = 1
      CALL D01GAF(X,A,II,ANS,ERROR,IFAIL)
      IF (IFAIL.GT.0) THEN
       IF (IFAIL.EQ.1) WRITE (6,99998)
       IF (IFAIL.EQ.2) WRITE (6,99997)
       IF (IFAIL.EQ.3) WRITE (6,99996)
      ENDIF
      D=ANS
      TIME=X(II)
      T=-Q/8.3143D+00*DLOG(D/TIME)
      WRITE(6,*) 'DE,TE =',D,T
C
99998 FORMAT (/' LESS THAN 4 POINTS SUPPLIED')
```

```
99997 FOMAT (/' POINTS NOT IN INCREASING OR DECREASING ORDER')
99996 FORMAT (/' POINTS NOT ALL DISTINCT')
99994 FORMAT (/' MORE THAN NMAX DATA POINTS')
      RETURN
      END
C ***************************************************************************
      DOUBLE PRECISION FUNCTION FUN(Q,T)
      IMPLICIT REAL*8(A-H,K-Z)
      DOUBLE PRECISION T(2)
      VA=SPECIMEN TRAVEL SPEED AT PEAK TEMPERATURE A
      VB=SPECIMEN TRAVEL SPEED AT PEAK TEMPERATURE B
      FUN=(VA/VB)-DEXP(-Q/8.3143D+00*DABS((T(1)-T(2)/(T(1)*T(2))))
      WRITE(6,*) 'Q, FUN=',Q,FUN
      RETURN
      END
```

APPENDIX FOUR

Differential Thermal Analysis

12.1 Introduction

Stored energy measurement experiments were also performed to confirm that much of the free energy stored in MA6000 in as-received condition is in the form of grain boundaries as would be expected for such a fine grained microstructure (see, chapter 4) and the free-energy stored in MA956 in as-received condition is in the form of dislocations. Differential thermal analysis (DTA) experiments were carried out on samples in as-received condition. This was to support the results obtained after characterisation of initial microstructure of alloys MA6000 and MA956, as discussed in chapter 4.

The DTA experiments infact appeared to be unsuccessful because, at the temperature (1160°C for MA6000) where recrystallisation was expected an absorption of heat was observed, whereas an evolution of heat was anticipated.

In this appendix the results obtained from the differential thermal analysis (DTA) carried out to measure the stored energy in as-received (hot-rolled) condition, for nickel base superalloys (MA6000) and ferritic steel MA956, and the methods adapted to calculate the grain boundaries energy and deformation energy are discussed.

12.2 Differential Thermal Analysis (MA6000)

The DTA experiments were performed to our design by ESAB laboratories in Sweden, due to unavailability of the required high temperature equipment in the Department. The interested DTA output data have been analysed to calculate the energy stored in MA6000 in the as-received condition. For calorimetric calibration purposes K_2SO_4 was used since its enthalpy (H) data have been thoroughly reported in the literature e.g., Barin and Knacke (1973), have reported enthalpies for the phases of K_2SO_4. Their data are reproduced in Table 12.1.

DTA experiments were first performed to caliberate the instrument using Potassium Sulphate. The calibration was carried out by observing the α to β transformation, which occurs at 590°C and which has associated with an enthalpy change of 0.05 J/mol (2.14 Kcal/mol, see Table 12.1).The

results of this are represented in figure 12.1, and permit a measured peak area to be converted into an enthalpy change. For all the experiments heating rate used was 5 K/min. The weight of the K_2SO_4 sample used was 100 mg, and the reference (weight = 1.3103 mg) consisted of a fully annealed sample of MA6000 (1300°C for 4 hours).

After the calibration was completed, the experiment was repeated by substituting an as-received sample of MA6000 (4mm diameter × 15mm long, and the sample weight was 1.537 mg) into the sample container. The results of this are presented in figure 12.2. Two rather diffuse endothermic peaks were observed, although the detailed reason for the observation of two peaks is unclear, and cannot be attributed to γ' dissolution since the DTA method takes the difference between a sample and a reference. Since the reference itself is MA6000 (annealed), γ' effects are absent in this output. Note that the temperature range over which the peaks are observed is consistent with the recrystallisation temperature reported by (Hotzler and Glassgow 1980, and Mino et al. 1984)

The measured value of stored energy was compared versus an estimated value of stored energy due to grain boundaries and energy of deformation by DTA, are reported in Table 12.2. The free energy stored for MA6000 was measured around 11.2 MJ/m^3, which is about equals to the energy stored in the grain boundaries calculated (11.0 MJ/m^3), These approximately equal values of the stored energy and energy stored in grain boundaries proves that all the free energy stored in the nickel base superalloy is in the form of grain boundary energy. The methods adapted to measure the stored energy by DTA, the grain boundaries energy and energy of deformation are defined in section 12.4 of this appendix.

12.3 Differential Thermal Analysis (MA956)

Differential thermal analysis experiments using the procedure described earlier, was used to measure the stored energy of a sample of MA956 (weight 1.3034mg) in the as-received condition, at a heating rate of 5 K/min.

During annealing, MA956 samples were found to recrystallise at 1180°C during both isothermal and zone annealing experiments, but during continuous heating at 5 K/min., no DTA peaks were observed until a temperature of about 1530°C was reached. This could be a consequence of some dynamic recovery during heating in the DTA experiment, an effect which would be expected to retard recrystallisation (this is consistent with the pre-annealing experiments reported in the thesis).

The results obtained from the differential thermal analysis for MA956 are listed in Table 12.2. It can be seen that the stored energy (218.0 MJ/m^3) is much higher than the measured value for the nickel base superalloy MA6000 and only a small part of this appears to be due to grain boundary energy. The differential thermal analysis results need detailed confirmation, but unfortunately, they could not be repeated since the apparatus was not readily accessible. In spite of this, it is clear that much higher stored energy is consistent with the observed highly deformed microstructure. Indeed, the microstructure of as-received MA956 can genuinely be described as being in the cold deformed state.

Consequently, the driving force for recrystallisation is very large when compared with MA6000, which in the as-received state proved to be a primary recrystallised structure.

Table 12.1. Thermochemical properties of K_2SO_4, after Brain and Knacke (1973). Since the original table is not in the SI units and to avoid introducing rounding off errors, those units are preserved.

		A	B	C	D	Range
SOL-A	CP	28.77	23.80	-4.26		298-856
SOL-B	CP	33.60	13.40			856-1342
LIQ	CP	47.80				1342-1700

PHASE	T	CP	H	S	G	BT
SOL-A	298	31.074	-342.700	42.000	-355.222	260.420
	300	31.177	-342.642	42.193	-355.300	258.871
	400	35.627	-339.287	51.814	-360.013	196.728
	500	38.966	-335.552	60.134	-365.620	159.834
	600	41.867	-331.508	67.499	-372.008	135.522
	700	44.561	-327.186	74.157	-379.096	118.375
	800	47.144	-322.600	80.277	-386.822	105.689
	856	48.561	-319.920	83.514	-391.408	99.946
			2.14	2.500		
SOL-B	856	45.070	-317.780	86.014	-391.408	99.946
	900	45.660	-315.784	88.288	-395.243	95.991
	1000	47.000	-311.151	93.168	-404.319	88.376
	1100	48.340	-306.384	97.711	-413.866	82.239
	1200	49.680	-301.483	101.974	-432.852	77.204
	1300	51.020	-296.448	106.004	-434.253	73.014
	1342	51.583	-294.293	107.635	-438.739	71.460
			8.8	6.557		
LIQ	1342	47.800	-285.493	114.192	-438.739	71.460
	1400	47.800	-282.721	116.215	-445.422	69.543
	1500	47.800	-277.941	119.513	-457.210	66.624
	1600	47.800	-273.161	122.598	-469.317	64.114
	1700	47.800	-268.381	125.495	-481.723	61.938

Symbols and abbreviations used in the Table 12.1.

A, B, C, D	Temperature coefficient in the equations for the molar heat CP and decimal logarithm of the vapour pressure LP
CP	Molar heat cal/mol/degree
BT	β function; β (T) = - 10^3 G(T) / 4.575 T
G	Free energy in kcal/mol
H	Enthalpy in kcal/mol
LIQ	"liquid phase"
S	Entropy in cal/mole/degree
SOL-A	α phase
SOL-B	β phase
T	Temperature in K

Table 12.2. Stored energy measured by differential thermal analysis (DTA), calculated grain boundaries energies and energy of deformation for ODS superalloy MA6000 and ODS ferritic steel MA956. Methods used to calculate stored energy in grain boundaries and work of deformation, are discussed in the following section.

Material	Stored Energy Measured by DTA MJm^{-3}	Energy Stored in Grain Boundaries MJm^{-3}	Work of Deformation MJm^{-3}
MA6000	11.2	11.0	140.0
MA956	218.0	0.2	48.0

12.4 Methods For DTA Results Analysis

The stored free energy, energy stored in the grain boundaries and work of deformation were measured by the analysis of DTA results by following methods:

1. Stored free energy

To measure the free energy stored in the material , enthalpy (H) of the substance used for the caliberation of equipment has to be known. In the present work K_2SO_4 have been used for DTA experiments performed on the two ODS alloys MA6000 and MA956.

The enthalpy (H) for K_2SO_4 at 540 °C is reported in the literature as 2.14 kcal/mol (Brain and Knacke, 1973 and also see Table 12.1). Since the weight of sample and reference was measured in grams and milligrams respectively, so for the convenience of calculations the units kcal/mol have been converted to kJ/gram, using following conversion factors:

4.187 Joules = 1 calorie

174.26 grams = 1 mole (Smithells ,1983).

Finally the value of enthalpy (H) for K_2SO_4 was obtained as,

$$H = 0.051 \text{ kJ/gram}$$

The stored free energy was then measured as follows:

$$\Delta H_R = A_{sp} / W_s / A_{rp} / W_r \times H \text{ J/gram} \qquad (12.1).$$

where,

ΔH_R	heat of recovery per gram
A_{sp}	area under DTA peak for sample
W_s	weight of sample
A_{rp}	area under DTA peak for reference
W_r	weight of reference

and finally,

$$\Delta H_R^V = \Delta H_R \times \text{Density} = \text{Stored Free Energy J/m}^3 \qquad (12.2)$$

where, ΔH_R^V is heat of recovery per unit volume.

The stored free energy measured by DTA is given in Table 12.2 and the values measured for the above variables to calculate the stored free energy are given in Table 12.3. The values listed under density column are taken from Incomap data sheets for alloys MA6000 and MA956.

Table 12.3.

Material	A_{sp} mm^2	W_s grams	A_{rp} mm^2	W_r mg	ΔH_R J/gram	Density g/m^3
MA6000	179.8	1.5378	430	100	1.380	8.11×10^6
MA956	2494.8	1.3288	315	50	30.397	7.2×10^6

2. Energy stored in grain boundaries

From the values of measured stored free energy, the amount of energy stored in the grain boundaries was calculated by assuming that all the energy measured is stored as the grain boundary energy.

$\therefore$ $$S_{v\sigma} = \text{Stored free energy J/m}^3$$

and $$S_v = 2\sigma / L \qquad (12.3)$$

where,

S_v	is interface energy
σ	is grain boundary energy per unit area $\cong$ 0.5 J/m^{-2}
L	grain size (5×10^{-6})

3. Work of deformation

To calculate the energy of deformation it is essential to know the yield strength of the material at hot working temperature. The yield strength can be calculated at certain temperature, if the yield strength of the material is known at the lower and higher temperatures than the certain temperature (in this case the hot-rolling temperature). The following procedure was applied to calculate the yield

strength of the ODS alloy MA6000 only, because the yield strength for MA956 at hot-rolling temperature (1000°C) is mentioned in Incomap data sheet for Incoloy alloy MA956.

$$\sigma_Y = \sigma_Y \{T_O\} - T_{REQ} - (T_O / T_H) - T_O \times \sigma_Y \{T_O\} - \sigma_Y \{T_H\} \qquad (12.4)$$

where,

$\sigma_Y \{T_O\}$	yield strength at lower temperature = 344 MPa
$\sigma_Y \{T_H\}$	yield strength at higher temperature = 192 MPa
T_O	lower temperature = 982 °C
T_H	higher temperature = 1093 °C
T_{REQ}	Temperature required = 1040 °C

Since the yield strength at required temperature, which is 1000 °C (hot-rolling temperature) for Incoloy alloy MA956 is reported in Incomap booklet, so the values given above are only for Inconel alloy MA6000 and are taken from the Incomap brochure supplied with the alloy. After calculating yield strength at the temperature at which hot rolling carried out, it is possible to workout the energy of deformation simply by multiplying the calculated yield strength by the amount of deformation in terms of reduction in area. Since it is very well known that during hot rolling operations only 5% of the energy retain in the material as stored free energy and rest of it is dissipated as heat. Therefore, the calculated energy of deformation as given in Table 12.2 is only the 5% of the total energy calculated.

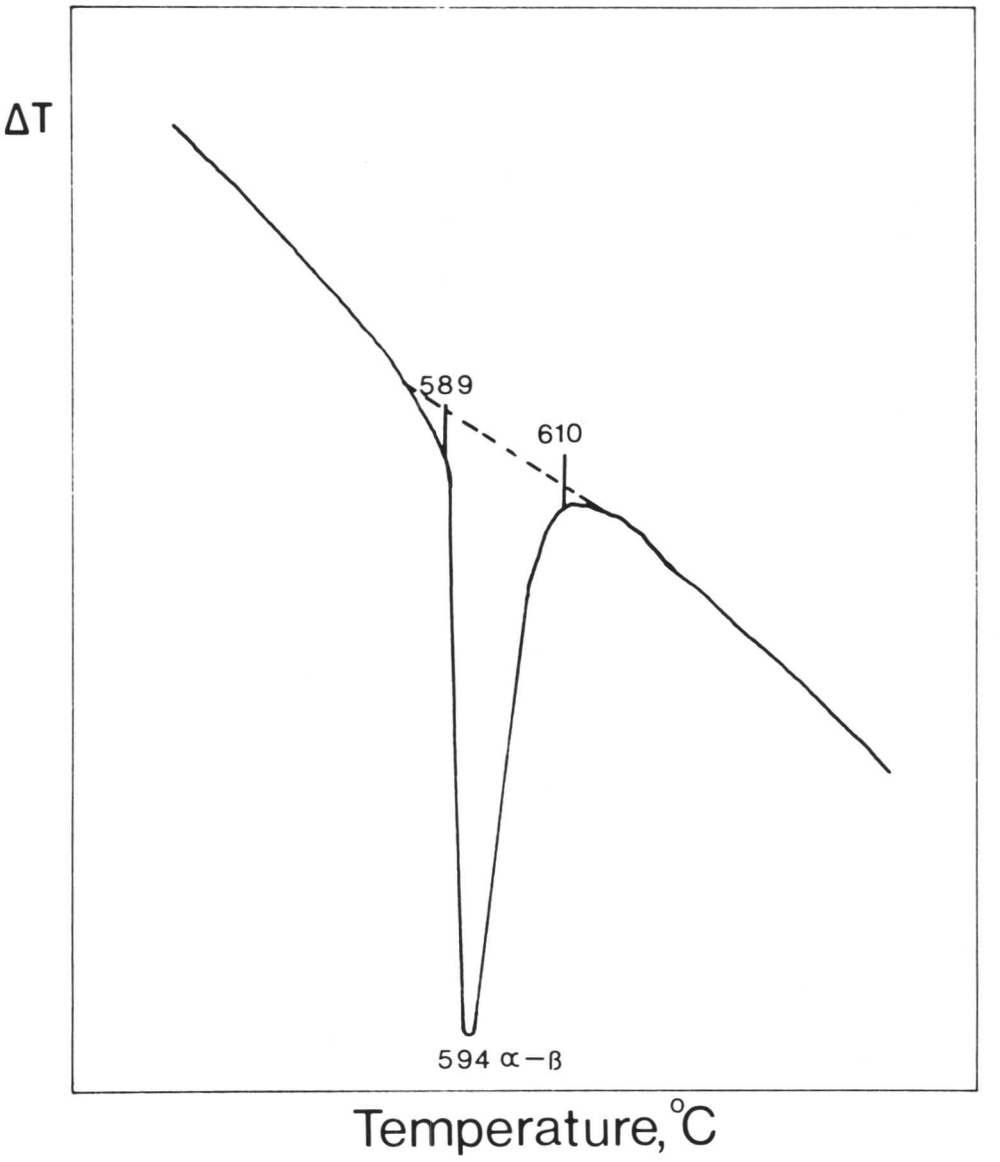

Figure 12.1. Differential thermal analysis curve observed for K_2SO_4 from α to β transformation, where the weight of the sample is equal to 100mg and a heating rate of 5 K/min was used. Line under DTA peak represent the base-line considered to calculate area under peak.

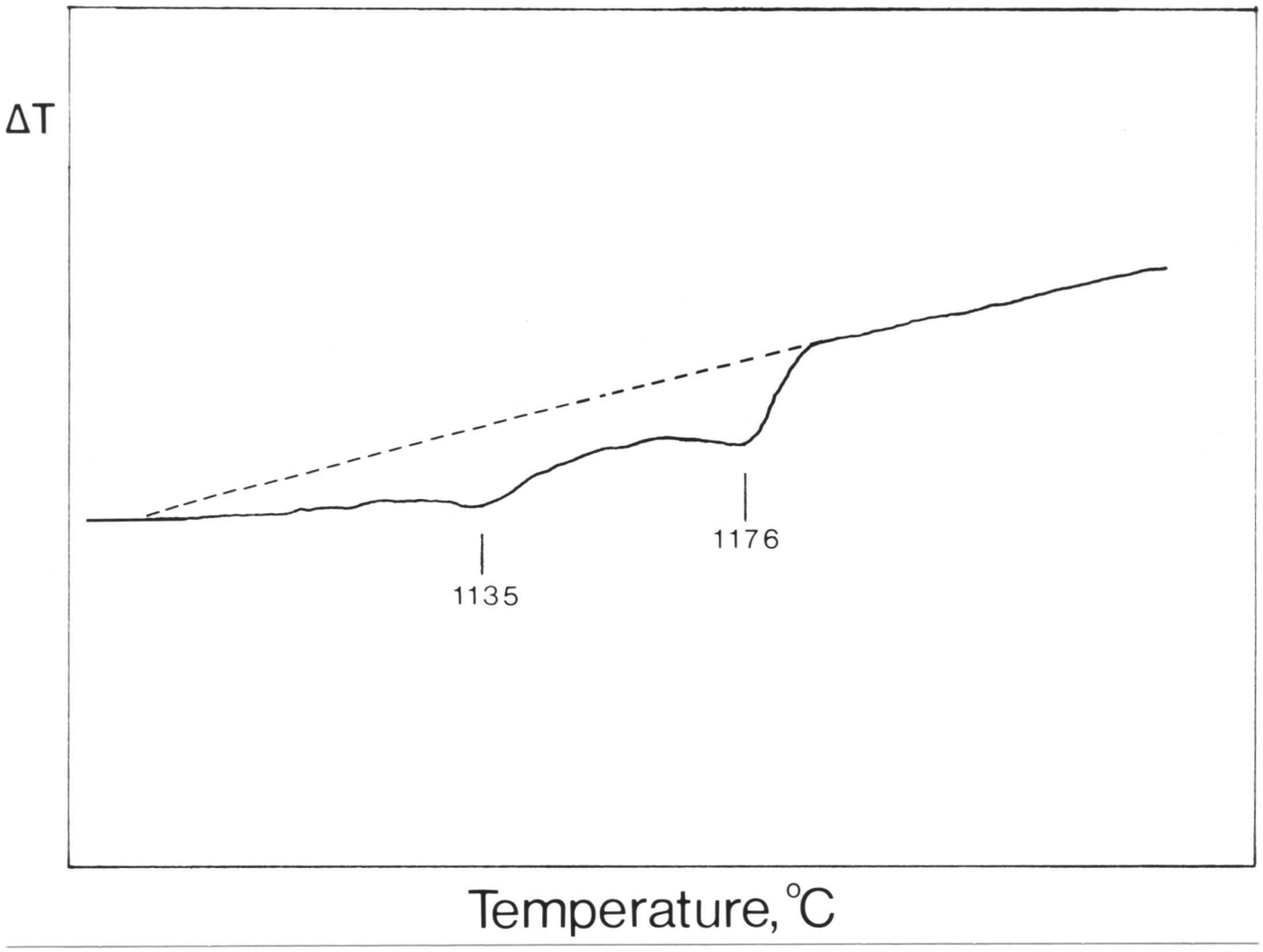

Figure 12.2. Differential thermal analysis curve observed for nickel base superalloy MA6000 at 1135-1176°C. Peaks are considered to be due to recrystallisation during differential thermal analysis. The weight of the sample was equal to 1.537mg and a heating rate of 5 K/min was used. Line under DTA peak represent the base-line considered to calculate area under peak.

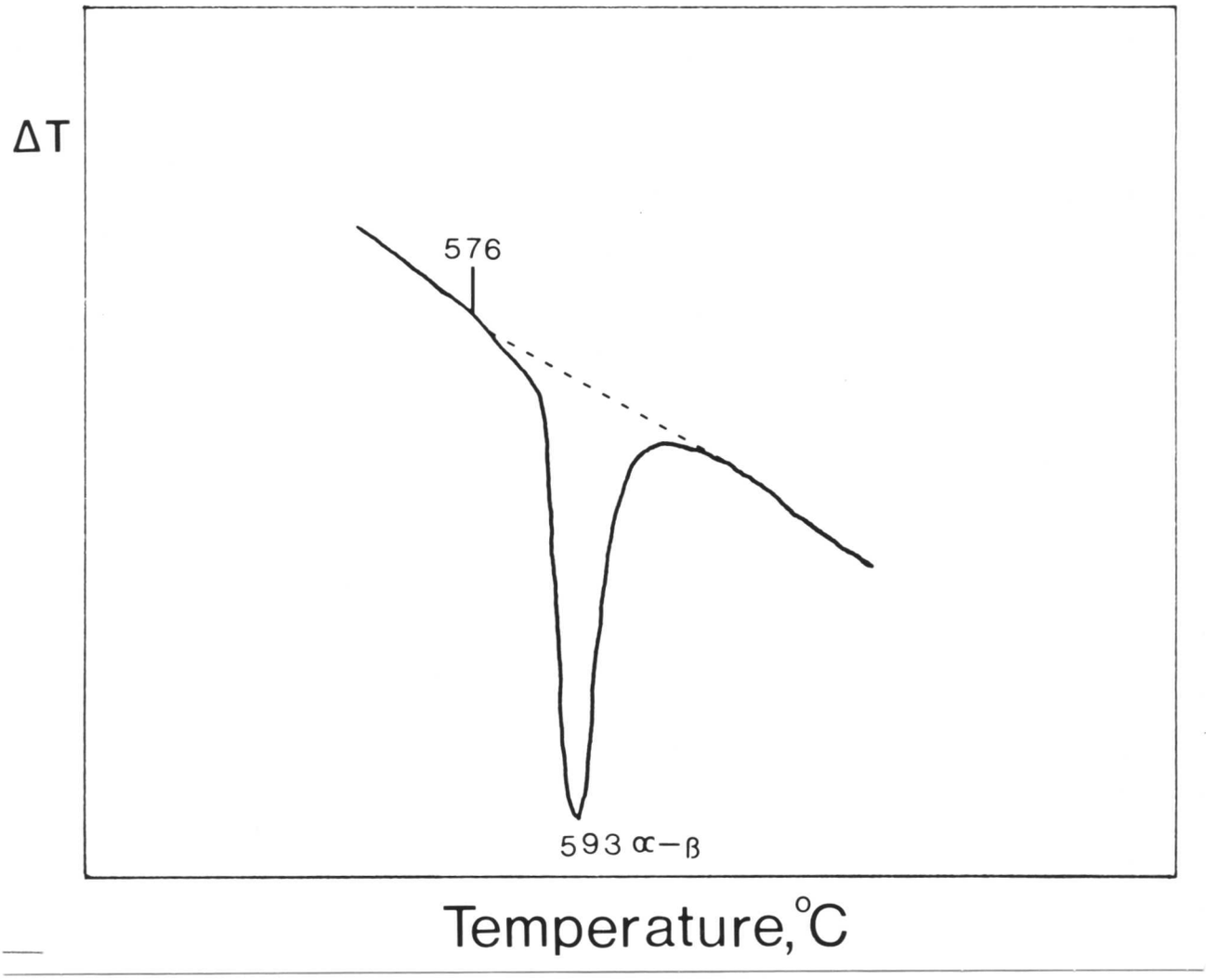

Figure 12.3. Differential thermal analysis curve observed for K_2SO_4 from α to β transformation, where the weight of the sample is equal to 50mg and a heating rate of 5 K/min was used. Line under DTA peak represent the base-line considered to calculate area under peak.

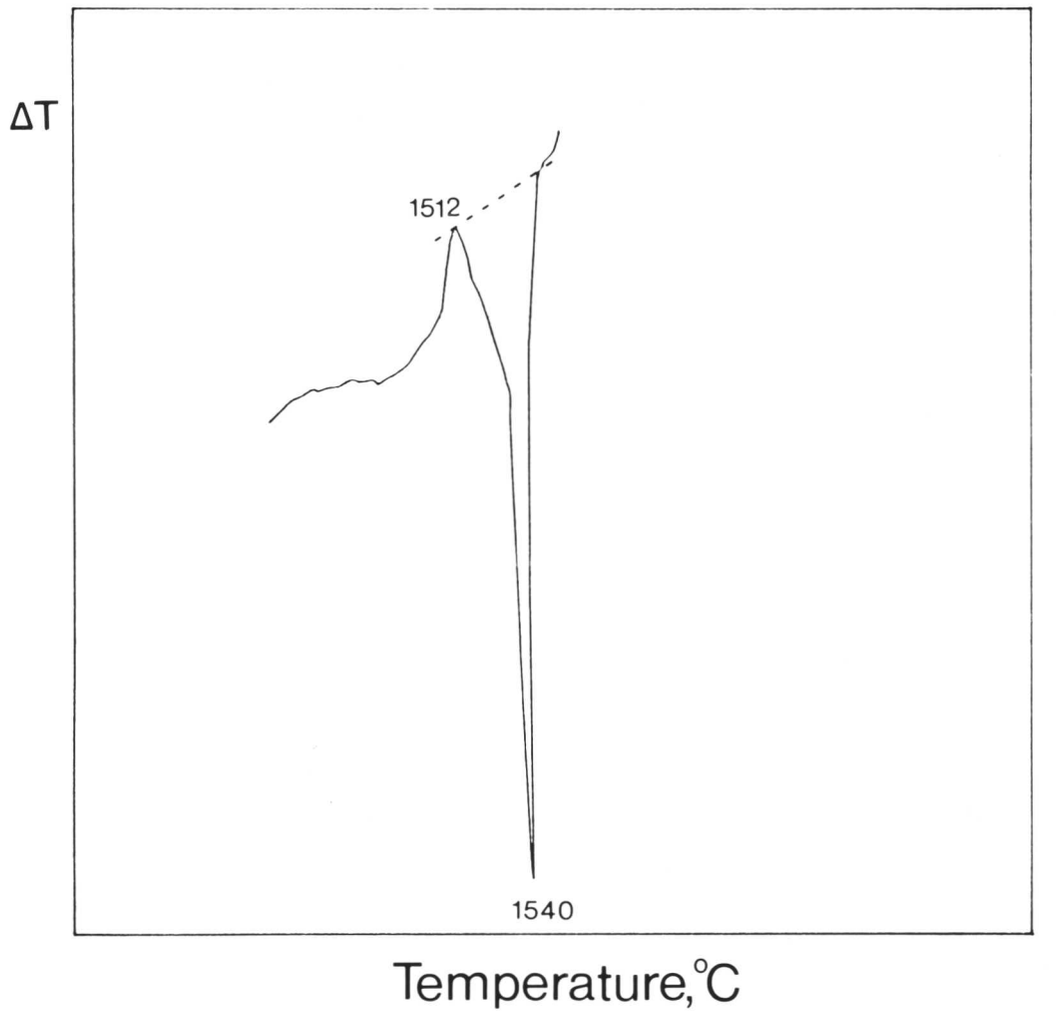

Figure 12.4. Differential thermal analysis curve observed for ODS ferritic steel MA956 at 1540°C. The peak shown for MA956 in above figure is reduced to two and half times, compared with the original peak observed during differential thermal analysis. The weight of the sample was equal to 1.3034mg and a heating rate of 5 K/min was used. Line under DTA peak represent the base-line considered to calculate area under peak.

References

Allen, M. M., Miller, J. A., and Woodings, B. E. (1976) US Patent no 3,975,219.

Artz, E., and Singer, R. F. (1984), in "Superalloys 1984." ed. by M. Gel et al. ASM, Ohio, p. 367.

Ashby, M. F., and Easterling, K. E. (1982), Acta Metall., vol. 30. p. 1969.

Aust, K. J., and Rutter, J. W. (1959), Trans. AIMME, vol. 215, p. 820.

Aust C. T. (1963), chapter 23 in "The Art and Science of Growing Crystals", J. J. Gilman, ed., John Wiley and Sons, NewYork, N. Y.

Avrami, M. (1939), J. Chem. Phys., vol. 7, p. 1103.

Avrami, M. (1940), J. Chem. Phys., vol. 8, p. 212.

Avrami, M. (1941), J. Chem. Phys., vol. 9, p. 177.

Barin, I., and Knacke, O. (1973), Thermochemical Properties of Inorganic Substances, Pbls. Springer-Verlag, Berlin, p. 379.

Bay, B., and Hansen, N. (1979), Met. Trans. A, 10A, p. 279.

Been, R. C., Benjamin, J. C., and Austin, C. S. (1984), in "High Temperature Alloys"., Theory and Design, ed. J. O. Stiegler. Metallurgical Society of AIME, p. 419.

Bell, F., and Krisement, O. (1962), Z. Metallk., vol. 53, p. 115.

Bell, F. (1965), Acta Metall., vol. 13, p. 363.

Benjamin, J. S. (1970), Met. Trans., vol. 1, p. 2943.

Bhadeshia, H. K. D. H. (1983), Graduate Lectures on Thermal Analysis, University of Cambridge.

Bhadeshia, H. K. D. H. (1987), "Worked Example in the Geometry of Crystals". Institute of Metals. London, p. 80.

Bloch, E. A. (1961), Met. Rev., vol. 6, p. 193.

Byrne, J. G. (1965), Recovery, Recrystallisation and Grain Growth of Metals, eds. L. Himmel, Interscience, New York, p. 211.

Cahn, R. W. (1949), Proc. Phys. Soc., A63, p. 323.

Cahn, R. W. (1949), J. Appl. Phys., vol. 32, p. 525.

Cahn, R. W. (1950), J. Inst. Metals, vol. 76, p. 121.

Cahn, R. W. (1965), Physical Metallurgy, 1st ed. Publs. North Holland, Co. Amsterdam, p. 925.

Cahn, R. W. (1983), in "Physical Metallurgy, part 2." 3rd ed. eds. R. W Cahn and P. Hansen, Publs. North Holland, Amsterdam, p. 1595.

Cairns, R. L. (1974), Metall. Trans. vol. 5, p. 1677.

Cairns, R. L., Curwick, L. R., and Benjamin, J. S. (1975), Metall. Trans. A, 6A, p. 179.

Calvet, J., and Renon, C. (1960), MeM. Sci. Rev. Met., vol. 57, p. 347.

Christian, J. W. (1965), "Theory of Transformations of Metals and Alloys", 1st ed. vol. 1, Pregamon Press Ltd. Oxford, p. 710.

Christian, J. W. (1975), "Theory of Transformations of Metals and Alloys", Part 1, 2nd ed. Pregamon Press Ltd. Oxford.

Clarebrough, L. M.,Hargreaves, M. E., and West, G. W. (1955), Proc. Roy. Soc. vol. A232, p. 252.

Clarebrough, L. M.,Hargreaves, M. E., and Loretto, M. H. (1963), Recovery and Recrystallisation of Metals, Interscience, New York, p. 43. vol. A232, p. 252.

Clark, D. S., and Verney, W. R. (1962), Physical Metallurgy for Engineers, 3rd ed., Pbls. Van Nostrand Co. Inc., New York, p. 104.

Claudia, J. B., Sanford, B., and John, K. T. (1979), Metall. Trans. A, 10A, p. 1297.

Cotterill, P., and Mould, P. R. (1976), Recrystallisation and Grain Growth in Metals, Surrey University Press, London, p. 31.

Cottrell, A. H., and Aytekin, V. (1950), J. Inst. of Metals, vol. 77, p. 1257.

Cottrell, A. H. (1953), Dislocations and Plastic Flow in Crystals, p. 188.

Couper, M. J. (1984), in "PM Aerospace Materials", A Metal Powder Report Conf. Berne, Switzerland, p. 28.

Crowford, (1983), Proc. Conf. "Frontiers of high temperature materials II." eds.I. S. Benjamin & R. C. Benn. Inco alloys Int. London. p. 272: referenced by Singer & Artz (1986).

Dahlen, M., and Winberg, L. (1979), Met. Sci. p. 163.

Decker, R. F., and Freeman, J. W. (1960), Trans. Metal. Soc. AIME, vol. 218, p. 277.

Decker, R. F., and Sims, C. T. (1972), "The Superalloys", eds. C. T. Sims and W. C. Hagel, New York, p. 33.

Doherty, R. D., and Martin, J. W. (1962), J. Inst. Metals, vol. 91, p. 332.

Edington, J. W., Melton, K. N., and Cutler, C. P. (1976), Prog. in Mat. Sci. vol. 21, p. 61. "Superplasticity."

English, A. T., and Backofen, W. A. (1964), Trans. AIME, vol. 230, p. 396.

Erdos, E. (1983), in "Analysis of high temperature materials." ed. by O. Vander Biest, Appl. Sci. Publ. London, p. 189.

Fawley, R. W. (1972), in " The Superalloys", ed. by C. T. Sims and W. C. Hagel, New York, p. 3.

Fischer, J. J. Astley. I. Morse J. P. (1977), Proc. 3rd Int . Symp. on Superalloys: Metallurgy and Manufacture, p. 361.

Fleetwood, M. J., (1986), Mater. Sci. and Technol., 2, p. 1176.

Gessinger, G. H. (1984), "Powder Metallurgy of Superalloys." Butterworths, Cambridge. Chapter 7 & 8, p. 211.

Gilman, J. J. (1955), Acta Metall. vol. 3, p. 277.

Gilman, P. S., and Benjamin, J. S. (1983), Ann. Rev. Mater. Sci. vol. 13, p. 279.

Gordon, P. (1955), Trans. AIME, vol. 203, p. 1043.

Hack, G. A. J. (1984), Powder Metallurgy, vol. 27. No. 2. p. 74.

Hack, G. A. J. (1988), Metall. Trans. A, vol. 19A, p. 732.

Hansen, N., and Bay, B. (1972), J. Mater. Sci. vol. 7, p. 1351.

Herbst, P., and Huber, J. (1978), "Texture of Materials", eds. G. Gottstein and K. Luke, (Spring-Verlag, Berlin), vol. 1, p. 453.

Hibbard, Jr. W. A., and Dunn, C. G. (1957), Creep and Recovery, ASM, Cleveland, p. 52.

Hoffelner, W., and Singer, R. F. (1985), Metall. Trans. A, vol. 16A, p. 393.

Hollomon, J. H., and Jaffe, L. D. (1945), Trans. TMS-AIME, 162, p.223.

Holmes, E. L., and Wingard, W. C. (1959), Acta Metall. vol. 7, p. 411.

Holmes, E. L., and Wingard, W. C. (1960), J. Inst. of Metals, vol. 88, p. 468.

Holt, R. T., and Wallace, W. (1976), Int. Metals Rev. No. 203, p. 1.

Honeycombe, R. W. K. (1984), Plastic Deformation of Metals, IIed. Pbls. Edward Arnold, London, p. 287.

Hotzler, R. K., and Glasgow, T. K. (1980) Proceedings of Fourth International Symposium on Superalloys, p. 455.

Hotzler, R. K., and Glassgow, T. K. (1982), Metall. Trans. A, 13A, p. 1665.

Howson, T. E., Stulga, J. E., and Tien, J. K. (1980), Metall. Trans. A, 11A, p. 1599.

Huet, J. J., De-Wilde, L., and Leroy, V. (1979), Metallurgie X1X - 1/2, p. 37.

Hughes, I. R., Marshall, G. J., and Miller, W. S. (1985), Rapidly Quenched Metals V, eds. S. Steeb and H. Warlimont, Elsevier, p. 1743.

Humphreys, F. J., and Martin, J. W. (1967), Phil. Mag. vol. 16, p. 927.

Humphreys, F. J. (1977), Acta Metall. vol. 25, p. 1323.

Humphreys, F. J. (1979), Acta Metall. vol. 27, p. 1801.

Humphreys, F. J. (1980a), Proc. Conf. on Recrystallisation and Grain Growth of Multiphase and Particle containing Materials, p. 35.

Incomap Data sheet: Incoloy Alloy MA956.

Incomap Data sheet: Inconel Alloy MA6000.

Jena, A. K., and Chaturvedi, M. C. (1984), J. Mat. Sci. vol. 19, p. 3121.

Kane, R. H., McColvin, E. M., Kelly, T. J., and Davidson, J. M. (1984), Proc. Conf. "Corrosion 84", New Orleans, La, USA. National Association of Corrosion Engineers, Paper, 12.

Khulman, D., Massing, G., and Raffelsieper, J. (1949), Z. Metallk. 40, (7), p. 241.

Kim, Y-W., Griffith, W. M., and Froes, F. H. (1983), ASM, Metals Congress, Philadelphia, Paper 8305-048.

Knowles, D. M. (1989), Fracture and Fatigue in MMCs, Dissertation submited for the CPGS. University of Cambridge.

Koster, U. (1971), Recrystallisation of Metallic Materials, Seminar of the Institute fur Metallkunde of the University of Stuttgart, p. 215.

Kronberg, M. L., and Wilson, F. H. (1949), Trans. AIMME, vol. 185, p. 501.

Lawley, A. (1977), Intr. J. of Powder Met. and Powder Technol. vol. 13, p. 169.

Leslie, W. C., Michalak, J. T., and Aul, F. W., (1963), Iron and its Dilute Solid Solutions, eds. C. W. Spencer and F. E. Wernet, New York Interscience Pbls. p. 119.

Li, J. C. M. (1961), J. Appl. Phys. vol. 32, p. 525.

Lloyd, D. M., and Cooke, M. J. (1981), Metall. Mater. Technol. vol. 13, p. 516.

Macdonald , D. M. (1981), Proc. Conf. on "Frontiers of High Temperature Materials, New York, Incomap, p. 101.

Mackanzie, R. C.(1970), Differential Thermal Analysis, Pbls. Academic Press Inc Ltd. London, vol. 1, p. 12.

Maringer, R. E. (1980), SAMPE Quarterly, July, p. 30.

Markham, A. J. (1988), Ph.D. Thesis, University of Cambridge. "The diffusion brazing of

nickel-based ODS alloys."

Marshall, G. J., Hughes, I. R., and Miller, W. S. (1986), Mat. Sci. and Technol. vol. 2, p. 394.

Marshall, G. J. (1989), Alcan International Limited, Banbury Laboratory, UK. Private Communication.

Miller, W. S., and Palmer, I. G. (1985), Proc. European Materials Research Society, Fall Meeting, Strasbourg, November, p. 117.

Mino, K., Asakawa, K., Nakagawa, Y. G., and Ohtomo, A. O. (1984), Proc. Conf. "PM Aerospace Materials", Metal Powder report, Berne, Switzerland, Paper 18.

Mould, P. R., and Cotterill, P. (1967), J. Mater. Sci. vol. 2. p. 241.

Nembach, E., Schanzer, S., Schroer, W., and Trinckauf, K. (1988), Acta Metall. vol. 36, p. 1471.

Palmer, I. G., Thomas, M. P., and Marshall, G. J. (1988), "Dispersion Strengthened Aluminium Alloys", eds. Y-W. Kim and W. M. Griffith. The Minerals, Metals and Materials Soc. p. 217.

Paris, H. G., Billman, F. R., Cebulak, W. S., and Petit, J. I. (1980), Rapid Solidification Processing, Principles and Technologies II. Proc. of the 2nd Inter. Conf. on RSP, Reston, Virginia, USA. p. 331.

Pickens, J. R. (1981), J. Mater. Sci. vol. 16, p. 1437.

Ramswamy, F., and Ramakrishnan (1981), Trans. of Powder Metallurgy Assoc. of India, vol. 8, p. 83.

Rhines, F. N., and Patterson, B. R. (1982), Metall. Trans. A, vol. 13A, p. 985.

Ricks, R. A., Porter, J. A., and Ecob, R. C. (1983), Acta Metall. vol. 31, p. 43.

Robinson, M. L. (1982), Forming of Incoloy Alloy MA956 Sheet, New York, Incomap.

Rollason, E. C. (1961), Metallurgy for Engineers, IIIrd. ed. Edward Arnold Ltd. London.

Schilling, W. F. (1977), Proc. 3rd Int . Symp. on Superalloys: Metallurgy and Manufacture, p. 373.

Sims, C. T. (1984), Proc. of the 5th. International Symposium on "Superalloys", Seven Spring Mountain Resort, Champion, Pennsylvania, USA. p. 399.

Singer, R. F., and Gessinger, G. H. (1981), "2nd Riso International Symposium on metallurgy and Materials Science. eds. N. Hansen, A. Horsewell, T. Leffers, H. Lilholt, Riso National Laboratory, Roskilde, Denmark, p. 365.

Singer, R. F., and Gessinger, G. H. (1982), Metall. Trans. A, 13A, p. 1463.

Singer, R. F., and Artz, E. (1986), in " High Temperature Alloys for Gas Turbines and other Applications." eds. W. Betz et al, D. Reidel Publ. Corp. Dordrecht, Holland, p. 97.

Smithells, C. (1983), Metal Reference Book, Sixth Edition, ed. Brandes E. A., Butterworths, London.

Stoloff, N. S. (1972), "The Superalloys", eds. C. T. Sims and W. C. Hagel, New York, p. 79.

Thomas, M. P., Palmer I. G., and Backer C. (1986), ASM, Symposium on Rapidly Solidified Materials, Orlando, Florida, p. 1.

Thursfield, G., and Stowell, M. J. (1974), J. Mater. Sci. vol. 9, p. 1644.

Tietz, T. E., and Palmer, I. G. (1981), Advances in Powder Technol. ed. G. Y. Chin, ASM, Metals Park, Ohio, p. 189.

Titchener, A. L., and Bever, M. B. (1958), Prog. in Metal Physics, vol. 7, p. 247.

Ubhi, H. S., Hughes, T. A., and Nutting, J. (1981) Proc. Conf. on Frontiers of High Temperature Materials. NewYork. p. 33.

Vandermeer, R. A., and Gordon, P. (1963), Recovery and Recrystallisation of Metals, ed. L. Himmel, Interscience, New York, p. 211.

Weber, J. H. (1980), SAMPE Quarterly, July, p. 35.

Weast, R. C. (1976-77), Handbook of Chemistry and Physics, 57th. Edition, Pbls. CRC Press, INC. Cleveland, Ohio, USA.

White, J., Hughes, I. R., Willis, T. C., and Jordan, R. M. (1987), J. De Physique, C3, Suppl. 9, p. 347.

Whittenberger, J. D. (1978), Met. Trans. A. vol. 9A, p. 101.

Whittenberger, J. D. (1979), Met. Trans. A. vol. 10A, p. 1285.

Wilcox, B. A., and Clauer, A. H. (1972), in "The Superalloys" eds. C. T. Sims, W. C. Hagel, Wiley Interscience, New York, p. 197.

Willis, T. C. (1988), Met. and Mater. vol 6, p. 485.

Wilson, F. G., Knott, B. R., and Desforges, D. C. (1978), Met. Trans. A. vol. 9A, p. 275.

Yang, J. R., and Bhadeshia, H. K. D. H. (1989), Mater. Sci. and Technol. vol. 5, p. 93.